Evidence for millennial-scale interactions between Hg cycling and hydroclimate from Lake Bosumtwi, Ghana

Alice R. Paine[1,2*], Joost Frieling[1], Timothy M. Shanahan[3], Tamsin A. Mather[1], Nicholas McKay[4], Stuart A. Robinson[1], David M. Pyle[1], Isabel M. Fendley[1,5*], Ruth Kiely[6], William D. Gosling[6]

[1]Department of Earth Sciences, University of Oxford, UK, OX1 3AN
[2*]Department of Environmental Sciences, University of Basel, Bernoullistrasse 32, CH-4056 Basel, Switzerland
[3]Department of Earth and Planetary Sciences, University of Texas at Austin, Texas, USA
[4]School of Earth and Sustainability, Northern Arizona University, Flagstaff, Arizona, USA
[5]Department of Geosciences, Pennsylvania State University, University Park, PA, USA
[6]Institute for Biodiversity & Ecosystem Dynamics, University of Amsterdam, Amsterdam, Netherlands

Corresponding Author: alice.paine@unibas.ch
** current affiliation*

Changing hydrology impacts the biogeochemical cycling of elements such as mercury (Hg), whose transport and transformation in the environment appear linked to hydroclimate on diverse timescales. Key questions remain about how these processes manifest over different timescales and their potential environmental consequences. For example, millennial-scale Hg-hydroclimate interactions in the terrestrial realm are poorly understood, as few sedimentary records have sufficient length and/or resolution to record abrupt and long-lasting changes in Hg cycling, and the relative roles of depositional processes on these changes. Here, we present a high-resolution sedimentary Hg record from tropical Lake Bosumtwi (Ghana, West Africa) since ~96 ka. A coupled response is observed between Hg flux and shifts in sediment composition, the latter reflecting changes in lake level. Specifically, we find that the amplitude and frequency of Hg peaks increase as the lake level rises, suggesting that Hg burial was enhanced in response to an insolation-driven increase in precipitation at ~73 ka. A more transient, threefold increase in Hg concentration and accumulation rate is also recorded between ~13 and 4 ka, coinciding with a period of distinctly higher rainfall across North Africa known as the African Humid Period. Two mechanisms, likely working in tandem, could explain this correspondence: (1) an increase in wet deposition of Hg by precipitation and (2) efficient sequestration of organic-hosted Hg. Taken together, our results reaffirm that changes in hydroclimate, directly and/or indirectly, can be linked to millennial-scale changes in tropical Hg cycling, and that these signals can be recorded in lake sediments.

KEYWORDS: lacustrine, geochemistry, sediment, sapropel, organic, Africa

1. Introduction

Mercury (Hg) is a volatile and toxic metal released into the atmosphere as a result of natural processes (e.g., volcanism, geothermal activity, weathering; Edwards et al., 2021; Selin, 2009) and, more recently, human activities (e.g., industrial activities, mining, coal burning; Amos et al., 2015). Approximately 95 % of atmospheric Hg exists in gaseous elemental form (Hg^0). An atmospheric lifetime of up to 2 years permits its transport over long distances prior to removal by wet or dry deposition (Lyman et al., 2020). Once free gaseous (Hg^0) and/or oxidised (Hg^{II}) Hg has been deposited into the terrestrial environment, two sets of reactions become particularly important: (1) oxidation-reduction, and (2) methylation-demethylation (Branfireun et al., 2020). The reduction of Hg^{II} to Hg^0 can result in release back into the atmosphere. Hg^{II} can also be bound to organic matter (OM) or sulphides, and thus be sequestered and accumulated in sediments (Åkerblom et al., 2013; Hsu-Kim et al., 2013; Mason et al., 2000). Accumulation of Hg in the terrestrial environment is therefore a function of the balance between Hg removal from and re-emission to the atmosphere, and governed by the rate and intensity of different thermal, photo, and biogenic reactions (Bishop et al., 2020; Obrist et al., 2018).

The exchange of Hg between the terrestrial biosphere, hydrosphere, critical zone, and atmosphere are intrinsically coupled to climate. Changes in ecosystem Hg loading, overland transport, and methylation have all been directly linked to decadal-scale changes in global temperature and precipitation, and their associated shifts in terrestrial productivity, land-atmosphere exchange, and wildfire dynamics (Bishop et al., 2020; Li et al., 2020). However, studying the long-term natural Hg cycle presents several challenges. For example, the overwhelming increase in anthropogenic Hg fluxes in recent decades have substantially altered the environmental dynamics of this cycle, complicating assessment of how long-term climate change may alter its rate, intensity, and evolution (United Nations Environment Programme, 2018). Pre-industrial-age archives allow for clear comparison between natural and anthropogenic-driven changes in Hg cycling, and identification of regions that may be most vulnerable to the negative effects of these changes, and highlight the importance of understanding the long-term Hg cycle (e.g., Cooke et al., 2020; Segato et al., 2023).

1.1. Mercury cycling and hydroclimate.

The transport and transformation of Hg at the Earth's surface is linked to the hydrological cycle (Bishop et al., 2020; Selin, 2009). Water plays a direct role in the efficiency of both Hg deposition and re-emission. For example, changes in precipitation amount can influence the proportion of Hg removed from the atmosphere by wet versus dry deposition, with higher precipitation amounts generally corresponding to enhanced Hg deposition at the surface (Amos et al., 2015; Guédron et al., 2018). Elevated Hg concentrations have been measured in equatorial ocean surface waters corresponding to inter-annual peaks in precipitation, with general circulation model simulations suggesting that these are likely due to higher net Hg flux by wet deposition (Kuss et al., 2011; Soerensen et al., 2014; Sprovieri et al., 2010). Multi-year monitoring by the Global Mercury Observation System (GMOS) has similarly revealed distinct interannual differences in total wet

deposition of Hg, with the highest fluxes typically occurring in the wettest years (Leiva González et al., 2022; Sprovieri et al., 2017). Precipitation also facilitates Hg transport in terrestrial watersheds, with simultaneous increases in river discharge, surface runoff, and soil erosion during and after intense storm events all enhancing hydrological 'connectivity' between surface environments and feeder tributaries (Bishop et al., 2020). This enhances overland transport of Hg and other suspended materials, and subsequently their delivery to lake and near-shore marine sediments (Liu et al., 2021; Zaferani and Biester, 2021).

Water also plays an indirect role in drawdown and sequestration of Hg in aquatic environments. Systems that are particularly sensitive to changes in water balance (e.g., terrestrial lakes) are most likely to experience distinct, hydro-climate driven environmental changes that impact their internal Hg cycle (Branfireun et al., 2020). For example, changes in organic matter cycling between the catchment and the lake (Ravichandran, 2004), algal scavenging (Outridge et al., 2019), and early diagenesis (Frieling et al., 2023). A decline in the total water volume of a basin may also elicit a reduction in stratification (Woolway et al., 2020), where increased mixing would ventilate bottom waters and reduce organic-matter burial (Gulati et al., 2017). Conversely, a simultaneous increase in total water volume and nutrient influx may increase stratification and bottom-water anoxia to such an extent, that the system experiences a distinct increase in organic matter burial (Pilla et al., 2020). Studies have also found catchment and basin structure to be important when considering the extent to which sedimentary Hg signals reflect hydroclimate-driven variability, as both influence how easily water is able to transport Hg to, from, and between discrete terrestrial sinks (Paine et al., 2024).

In the short-term, variability in hydroclimate may manifest as annual changes in rainfall intensity and seasonality, or by sub-decadal fluctuations in regional-scale climate modes (e.g., El-Nino Southern Oscillation, North Atlantic Oscillation; Hernández et al., 2020). In the long-term, variability in the form of prolonged droughts and/or pluvials may occur in response to global-scale atmospheric reorganization lasting centuries, and changes in the planet's orbital configuration on timescales of many millennia (Bradley and Diaz, 2021). These wet-dry oscillations are important on a continental-scale. For example, periods of extreme hydroclimate variability are known to have caused major changes in environmental conditions across sub-Saharan Africa during the late Pleistocene, lasting for multiple millennia (e.g., Scholz et al., 2007).

Millennial-scale changes in hydroclimate may also affect the Hg cycle. Sediment cores extracted from the Pacific and Atlantic oceans show low-amplitude Hg signals corresponding to orbital-scale (>10^4-year) changes in precipitation and rates of sediment delivery to the ocean (e.g., Chede et al., 2022; Fadina et al., 2019; Figueiredo et al., 2022; Zou et al., 2021), and a growing number of terrestrial successions also show Hg fluctuations coeval with climate-driven changes in local precipitation, cloud formation, and ice/permafrost extent (e.g., Guédron et al., 2018; Nalbant et al., 2023; Paine et al., 2024; Pan et al., 2020; Pérez-Rodríguez et al., 2018). However, few terrestrial Hg records extend beyond the present interglacial (>12 ka), and even fewer come from the low-latitudes, where tropical rainforest, grassland and desert biomes are highly sensitive to millennial-scale hydroclimate variability (Bradley and Diaz, 2021; Schneider et al., 2023). Thus, our current understanding of Hg behaviour

may not fully account for the impact of major, long-term hydroclimate changes on Hg transformation and transport through tropical environments (Obrist et al., 2018; Schneider et al., 2023), highlighting the need for new Hg records spanning long (>10^3-year) timescales.

1.2. Research objectives

Sedimentary records offer an opportunity to assess the impact of millennial-scale hydroclimate variability, and related effects, on the terrestrial Hg cycle. In sub-Saharan Africa, the West African Monsoon (WAM) regulates precipitation amount and distribution, and drives long-term evolution of environmental characteristics and mineral-dust emissions (Kaboth-Bahr et al., 2021; Kuechler et al., 2013; O'Mara et al., 2022; Weldeab et al., 2007). Proxy records from this domain show that orbitally-driven variations in the strength of the WAM have frequently driven distinct arid (Cohen et al., 2007; Scholz et al., 2007) and humid periods (Armstrong et al., 2023; Menviel et al., 2021) throughout the Pleistocene. These humid and arid periods have been linked to distinct changes in vegetation structure, ecosystem dynamics, and human evolution across the continent (e.g., Cohen et al., 2022; Foerster et al., 2022; Gosling et al., 2022b). In light of growing evidence for a hydroclimatic influence on the terrestrial Hg cycle (e.g., Guédron et al., 2018; Nalbant et al., 2023; Paine et al., 2024), we hypothesized that humid and/or arid periods in sub-Saharan Africa would have elicited measurable changes in the Hg cycle, producing measurable signals in regional sedimentary records. Here our focus is on sediment core BOS04-5B extracted from Lake Bosumtwi, Ghana (West Africa): a core that provides a clear and continuous record of this hydroclimate variability covering the late Pleistocene (Koeberl et al., 2007).

Lake Bosumtwi is a closed system isolated from the regional groundwater network, rendering it sensitive to both short- and long-term variability in rainfall, humidity, and dynamic surface processes (Shanahan et al., 2008b; Turner et al., 1996). Integrated proxy data shows that Lake Bosumtwi experienced dramatic changes in water balance, aeolian dust inputs, and biological productivity throughout its history. These changes all correspond to moisture-driven oscillations between a forest and grass-dominated catchment in response to insolation-driven variability in WAM strength, and migration of the Intertropical Convergence Zone (ITCZ) (Gosling et al., 2022a; Miller et al., 2016; Peck et al., 2004; Vinnepand et al., 2024). Focussing on the uppermost ~47 m of the Lake Bosumtwi sediment record, this study assesses whether major shifts in local hydroclimate produced measurable changes in how Hg has been transported to, and buried within, this system since ~96 ka. By comparing our sedimentary Hg record with proxy data from archives across the African continent (e.g., Foerster et al., 2022; Scholz et al., 2007), we explored whether hydroclimate has exerted a measurable effect on terrestrial Hg cycling in the WAM domain in over the past ~100-kyr.

2. Site Description

2.1. Lake Bosumtwi

Lake Bosumtwi is the only natural lake in Ghana, West Africa (6°30' N, 1°25' W) (**Fig. 1**). It occupies a meteorite impact crater dated to 1.08 ± 0.04 Ma, which is one of the youngest and best preserved impact craters on Earth (Jourdan et al., 2009). The surrounding bedrock and meteorite impact target rocks are Proterozoic metagraywackes, phyllites and metavolcanic rocks of the Birimian Supergroup (~2 Ga) (Jones et al., 1981). Lake beds, soils, and breccias constitute the most recent rock formations at the site, and are associated with evolution of the crater through time (Koerberl et al. 2007). The present-day lake is ~8.5 km in diameter with a water depth of up to 80 m at the centre, and the current water level is at least 120 m below the crater rim (Shanahan et al., 2007). The crater itself is ~10.5 km in diameter at the rim with steep slopes, and a well-defined spillway (~120 m above the present lake surface) marks evidence of lake overflow likely during the most recent humid period (**Fig. 1**) (Shanahan et al., 2015). The lake is meromictic, with a shallow oxycline located ~10–15 m below the water's surface (Turner et al., 1996).

The Bosumtwi basin is hydrologically closed with no external drainages, connection to the regional groundwater aquifer, river or stream inflow originating outside of the crater (**Fig. 1**) (Turner et al., 1996). Only during exceptionally high lake levels does water leave the lake, through the spillway (Shanahan et al., 2007). Approximately 300 m of sediment has accumulated in the centre of the basin originating from biological processes within the lake, progressive erosion of the crater wall, aeolian transport, and vegetation within the crater (Koeberl et al., 2005). These properties render the lake highly sensitive to changes in atmospheric processes, but also imply that Hg inputs may originate exclusively from the atmosphere (e.g., by wet deposition). Therefore, this system is ideally suited for exploring whether specific basin characteristics (e.g., depth, nutrient status, bathymetry) could also measurably affect how Hg signals are encoded in the sedimentary record.

2.1.1. West African Climate

Seasonal variability in the tropical rain belt position drives short-term hydroclimate change in West Africa. During boreal summer, an increase in northern hemisphere summer (June to August) insolation triggers a northward ITCZ shift, creating a pressure gradient that brings moisture eastwards from the Atlantic Ocean to western Africa. The opposite occurs in boreal winter (December to February), where the ITCZ is displaced southwards, bringing dry, aerosol-rich, continental trade winds to West Africa. Together, these seasonal shifts produce distinct annual wet (May to October) and dry seasons.

On longer (>10^4-year) timescales, hydroclimate variability in West Africa has been linked to cyclic changes in Earth's orbital configuration. Changes in axial precession produce fluctuations in seasonal insolation above the African continent, influencing the strength of the WAM, the Walker Circulation, the position and dimensions of the ITCZ, and the availability of continental moisture (Gosling et al., 2022b; Kaboth-Bahr et al., 2021; Trauth et al., 2021). Several studies have shown weakening of the

WAM and southward migration of the ITCZ in response to high precession and/or changes in insolation gradient, producing drier conditions in West Africa and subsequent reductions in terrestrial precipitation, ecosystem productivity, and recession of terrestrial forests . Conversely, strengthening of the WAM and a more northerly ITCZ position is documented when precession is low, bringing wetter and warmer conditions to West Africa and causing expansion of dense forests, voluminous lakes, and diverse ecosystems (Larrasoaña et al., 2013; Pausata et al., 2020). During the last glacial cycle, moisture availability in West Africa also fluctuated in conjunction with the waxing and waning of high-latitude ice sheets, and their effects on sea-surface temperatures (SSTs) in the North Atlantic (deMenocal, 1995; Weldeab et al., 2007). This teleconnection exists as a function of atmospheric moisture transport and convection processes occurring in the polar and tropical regions. Low global ice volumes typically correspond to warmer North Atlantic SSTs, driving increased atmospheric moisture transport and hence more moist conditions in West Africa. Conversely, high global ice volumes generally correspond to cooler SSTs in the North Atlantic, and subsequently drier conditions in West Africa (e.g., Crocker et al., 2022; Lupien et al., 2023; Stager et al., 2011; Tjallingii et al., 2008).

2.1.2. Local hydrology and vegetation

Approximately 49% of the Bosumtwi drainage basin (area: 106 km^2) is currently occupied by the lake. Situated in close proximity to the (current) ecological transition-zone between savannah in the north and moist forest in the south, Lake Bosumtwi lies directly in the seasonal migration path of the ITCZ (Nicholson, 2013). It experiences a current mean annual temperature of ~26^{o}C, ranging between ~23^{o}C in August to ~27^{o}C in February, with cooler temperatures attributed to increased cloudiness and related reduction in incoming solar radiation (Shanahan et al., 2007). Present-day humidity ranges from ~85% in August to ~75% in January, and average annual precipitation is ~1450 mm (Turner et al., 1996). At present, the surrounding catchment as classified as a '*Tropical and Subtropical Moist Broadleaf Forest'* biome (White, 1983), meaning it is heavily forested with well-developed tropical soils, although many flat-lying areas have been converted to agriculture (e.g., maize, plantain, cocoa, and oil palm) in recent decades (Boamah and Koeberl, 2007). Before human occupation of the site, the lake was surrounded by a moist semi deciduous forest, with a canopy including an abundance of trees from the Ulmaceae and Sterculiaceae (flowering plant) families (Miller and Gosling, 2014).

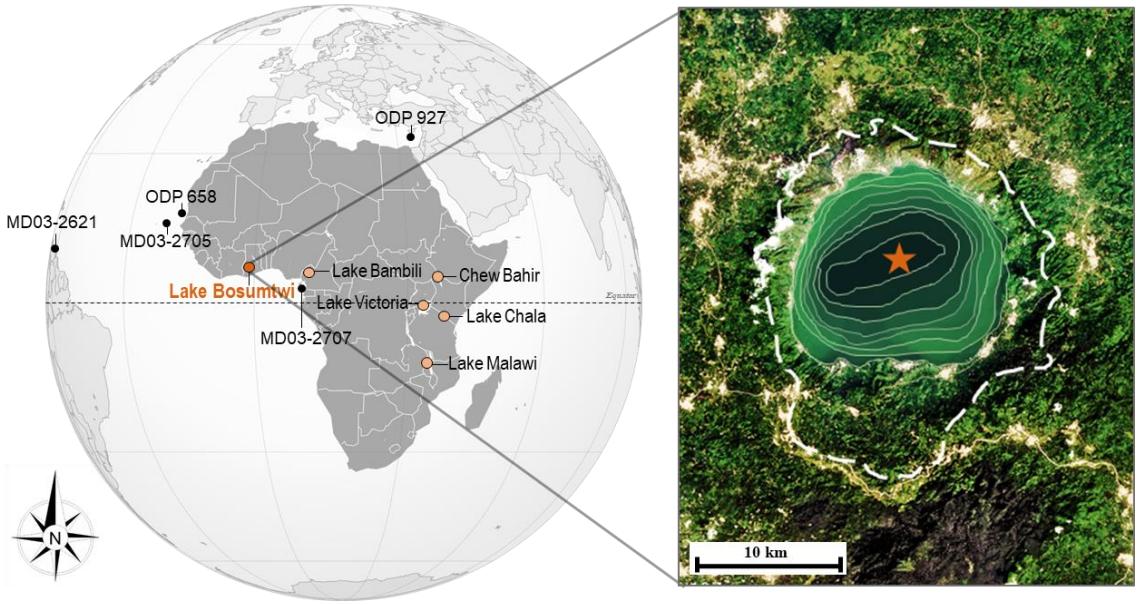

Figure 1: (Left) Location of key lake and marine sediment archives in and around Sub-Saharan Africa (SSA). (Right) An aerial photograph of Lake Bosumtwi (*copyright*: NASA, 2018), with the location of the BOS04-5B drill site marked as an orange star. Contours show lake bathymetry, with each step representing a 10 m depth change and culminating in a maximum depth of 75 m (Shanahan et al., 2012). The spillway notch is in the eastern rim of the crater, and the dashed white line marks the extent of the drainage divide (Brooks et al., 2005; Shanahan et al., 2006).

2.1.3. Paleoclimatic significance

Lake Bosumtwi provides an excellent record of millennial-scale hydroclimate change in West Africa. The upper ~47 m of sediment corresponds to the interval ~96 ka to present, and contains a series of distinct lithological features suggesting pronounced, climate-driven changes in lake level, catchment structure, and sediment transport processes (Vinnepand et al. 2024; Gosling et al., 2022a; McKay, 2012; Miller et al., 2016). For example, a massive, clastic-rich blue-grey clay unit is present between ~34 and 32 m depth, where TOC values drop to <1% and bulk density values increase by >60% (Scholz et al., 2007). Interpreted and referred to as Arid Interval(AI)-1 (McKay, 2012), this unit formed during extremely dry climatic conditions leading to near-total desiccation of the lake, and this interpretation is further supported by identification of a clear erosional unconformity corresponding to the age of the AI-1 unit in seismic reflection profiles (Brooks et al., 2005; Scholz et al., 2007).

Changing physical properties and geochemistry of sediments deposited prior to and following Unit AI-1 appear to reflect regional hydroclimate shifts (Scholz et al., 2007). Prior to AI-1, the presence of clastic-rich, organic-depleted sediments suggest a progressive reduction in water depth, likely in response to a (long-term) negative water balance (McKay, 2012; Shanahan et al., 2008b). Following AI-1, an abrupt reduction in clastic material concentrations, increased TOC, diagenetic carbonate, and lamination frequency all imply oxygen depletion at the sediment-water interface – evidence for a shift to a positive water balance (McKay, 2012; Scholz et al., 2007; Shanahan et al., 2008a). The core also shows distinct co-enrichment in manganese (Mn) and iron (Fe) in certain intervals following AI-1, that

are associated with manganosiderite (Mn-rich $FeCO_3$) precipitation in the lake sediments. Manganosiderite requires anoxic non-sulphidic (ferruginous) pore-water conditions and high dissolved inorganic carbon concentrations to precipitate (Brumsack, 2006; Tribovillard et al., 2006), and appears as a consequence of the redox tower migrating into the water column: a response to increasing water column stratification, and overall lake level (Shanahan et al., 2006). The closed hydrology of Lake Bosumtwi means that changing water levels will primarily reflect the magnitude of precipitation variability in the region, with higher lake levels typically occurring during wetter climate intervals (Russell et al., 2003; Shanahan et al., 2008b). However, lake level may have also been influenced by secondary processes such as evaporation, and, over long time-scales, sediment infill (McKay, 2012)

3. Material and methods

3.1. BOS04-5B

Core BOS04-5B was recovered in 2004 as part of the International Continental Drilling Program (Koeberl et al., 2005) (full details in **ST1**). Our study focuses on the upper ~47 m section of a 296-m-long core extracted from deep-water (76 m) site 5 (core BOS04-5B; **Fig. 1**), that extends from the present-day lake floor to the brecciated bedrock dated by $^{40}Ar/^{39}Ar$ to 1.08±0.04 Ma (Jourdan et al., 2009). Over ~67% of the full 294 m-long (~1-Myr) sediment succession is laminated (Koeberl et al., 2007), with distinctive alternating clastic, organic and carbonate laminae (Shanahan et al., 2012, 2009, 2008a). Thicker laminations are visible either as packets of light grey microturbidites, or distinct yellow and orange carbonates produced by enhanced redox-related precipitation of Fe and Mn bearing minerals (Shanahan et al., 2008a).

After drilling in 2004, core BOS04-5B was shipped to the University of Rhode Island and split. The physical properties of the full ~296 m core were measured at 2-cm intervals using a Geotek ® multi-sensor core logger (Koeberl et al., 2007). After logging and imaging and at 4-cm resolution, 2 cm thick slices were removed from the core half and separated into sub-samples for multi-proxy analyses, including sediment magnetic hysteresis, x-ray diffraction mineralogy, total organic and inorganic carbon content, bulk organic carbon and nitrogen isotopes, grain size, pollen, and charcoal (e.g., Gosling et al., 2022; McKay, 2012; Miller et al., 2016). Following bulk sediment analyses, the BOS04-5B core material was transferred to the Continental Scientific Drilling (CSD) Repository in Minneapolis.

3.2. Chronology

Age control for the ~47 m of sediment analysed in this study is provided by the BOSMORE7 model, presented by Gosling et al. (2022). Using a combination of radiocarbon (calibrated ^{14}C; n= 109), optically stimulated luminescence (OSL; n=22) and uranium-thorium (U/Th; n=5) dates as

independent tie-points, Bayesian modelling suggests that the upper ~47 m of sedimentation at Lake Bosumtwi corresponds to the interval ~96–0 ka (full details in **ST2**) (Gosling et al., 2022a; Shanahan et al., 2013). Age estimates for the AI-1 sedimentary unit are constrained by ^{14}C, OSL and U-Th dating of the surrounding sediments, and suggest this unit formed between 77 and 71 (±5) ka (Scholz et al., 2007; Shanahan et al., 2008b). The duration of the event is less clear due to the excessive erosion of the newly exposed crater walls and reduction in distance between the shore and 5B core site (McKay, 2012), and this process likely caused unusually high sedimentation rates during this interval. Thus, slight underestimation of sediment ages immediately following unit AI-1 may be expected.

3.3. Sediment geochemistry

3.3.1. Mercury

Total Hg (Hg_T) in the bulk sediments of core BOS04-5B was measured using the RA-915 Portable Mercury Analyzer with PYRO-915+ Pyrolyzer, Lumex (Bin et al., 2001) at the University of Oxford. For this study, we analysed 165 samples spanning the composite depth interval 47.7 to 0 m, with an average temporal resolution of ~0.6 ka between each sample (range: 0.01 to 5.85 kyr). Dry powdered sample material (45–100 mg) was heated to ~700°C, volatilizing Hg in the sample. Atomic absorption spectrometry of the gases produced during pyrolysis quantifies the total Hg content of the sample. Six different quantities of standard material (paint-contaminated soil – NIST Standard Reference Material ® 2587) with a known Hg value of 290 ± 9 ng g^{-1} were analysed to calibrate the instrument before sample analysis, and then one standard for every 10 lacustrine samples. Long-term observations of standard measurements *(n* = 390*)* for this instrument show average reproducibility (1 sigma) of 6% for samples with ≥10 ng g^{-1} Hg (Frieling et al. 2023). Four (2%) of the analysed samples contained very low Hg contents (<10 ng g^{-1}), and likely have uncertainties ≥10 %. Details of standard runs are included in an accompanying dataset.

3.3.2. Organic and inorganic carbon

Quantitative values for total organic carbon (TOC) and total inorganic carbon (TIC) content were measured on the same powdered sample material also analysed for Hg, using a Strohlein Coulomat 702 (Jenkyns and Weedon, 2013) at the University of Oxford. Analytical reproducibility for this instrument was ≤0.2 % based on repeat measurements, with a detection limit of ca. 0.1–0.2 %.

Powdered BOS04-5B sediment samples were split into two aliquots. Weights for aliquot 1 were between 50–70 mg, and aliquot 2 between 90–120 mg. Prior to coulometric analysis, aliquot 2 samples were furnaced for 24 hours at 420°C in order to remove organic carbon fractions. Both aliquots were then combusted in oxygen at 1220°C to break down the calcium carbonate and produce carbon dioxide (CO_2), that was fed into a solution of barium perchlorate. By producing a change in solution pH from an initial value of 10.0, back titration to the original pH using electrolysis provided a

measure of the amount of carbon originally present – quantified by the amount of electricity required to restore a pH of 10.0 and recorded in counts (Jenkyns, 1988; Jenkyns and Weedon, 2013). Counts obtained for aliquots 1 and 2 were used to calculate the total carbon (TC) content of each aliquot in wt.%, using the formula:

$$TC = \frac{total\ counts \times 0.2}{M} \quad \textit{(eqn. 1)}$$

where M is the sample mass in mg.

TOC was calculated as follows:

$$TOC = TC_1 - TC_2 \quad \textit{(eqn. 2)}$$

where TC_1 and TC_2 represent the TC values obtained for aliquots (1) and (2), respectively. TC_2 represents the TIC value for the sample. Our TOC curve was then compared with measurements previously obtained for BOS04-5B (on discrete samples): to assess the broader reproducibility of our results (**Fig. SF1**).

3.3.3. Authigenic carbonates

The BOS04-5B succession contains variable amounts of diagenetic carbonates, predominantly (mangano-)siderite (**Fig. SF2**) (McKay, 2012). Siderites commonly form in freshwater settings at shallow sediment depths under anaerobic (anoxic) conditions accompanied by organic-rich sediments (Armenteros, 2010; Sebag et al., 2018). However, they can also preclude accurate measurement of organic carbon content in lacustrine sediment via pyrolysis- or furnace-based methods, causing systematic overestimation of total organic carbon (TOC) due to the fact that thermal decomposition of siderite typically starts at temperatures <420^{o}C (Sebag et al., 2018): lower than the temperature used to remove the organic fraction on the Coulomat (Jenkyns, 1988). To assess whether siderite-associated carbon had an appreciable impact on the TOC measurements, we also analysed the carbon release from sixteen BOS04-5B samples spanning a range of low to high XRF-derived Mn counts (i.e., covering the possible range of (mangano-)siderite contents) using a weak acid (warm 5% HCl) treatment, following established methodologies (**ST5**; Brodie et al., 2011; Vindušková et al., 2019). Comparison of acid-treated and furnaced samples showed no systematic offset nor a clear correlation with the Mn counts from XRF data (**Fig. SF2c**), suggesting that the carbon release from siderite did not appreciably bias TOC measurements.

3.3.4. Scanning X-Ray fluorescence

The Hg data for core BOS04-5B generated in this study are paired with unpublished x-ray fluorescence (XRF) data for Si, Ti, K, Mn, Ca, Fe, Rb, Sr, S, and Al (McKay, 2012). The bulk elemental composition of the core was quantified using the Itrax® scanning XRF analyser at the

Large Lake Observatory at the University of Minnesota. Core material covering the upper ~159 m (~500-kyr) of BOS04-5B was analysed at 1-cm-resolution with 60 sec count times, and a Mo X-ray source run at 30 kV and 20 mA. To mitigate any effects arising from changes in the physical properties of the BOS04-5B sediments (e.g. compaction) and/or the measurement times, we applied a centred-log ratio (clr) transformation to the measured XRF values. The centred log-ratio (clr) values are calculated by dividing the intensities of an element by the average of the intensities obtained on all selected elements, and are dimensionless such that positive values are generated for elements with high intensities, and vice versa (Bertrand et al., 2024). Therefore, elements (X) subject to this transformation are presented as their centred-log ratio value (X_{clr}).

3.4. Mercury normalization

It is common practice to assess both total Hg concentration (Hg_T) and normalised Hg (Hg/X) with the aim to reduce, at least partially, the potential impact of variability in a dominant carrier/host phase (X) on Hg_T (Sanei et al., 2012; Shen et al., 2020). Organic matter (here expressed as TOC) is commonly considered the primary host phase of sedimentary Hg (Ravichandran, 2004). However, variability in Hg_T may also be associated with variability in the abundance of detrital minerals, usually detected by a correlation between Hg and detrital elements such as Al or K (Paine et al., 2024; Them et al., 2019), and very rarely in sulphate-limited (lacustrine) sediments, sulphides (Benoit et al., 1999; Han et al., 2008). Exploration of Hg signal variability relative to distinct shifts in the abundance, contribution and/or sources of host phases can therefore elucidate the timing and magnitude of shifts in lake hydrology, sedimentation regime, and geochemistry, and whether these are connected to changes in the Hg cycle or sediment composition changes (Paine et al., 2024).

To isolate the effects of local depositional and/or transport processes on Hg signals recorded in the sediments of Lake Bosumtwi, we normalised Hg_T values to organic matter (TOC) and detrital mineral abundance estimated from clr-transformed potassium intensities (K_{clr}); with the assumption that the strongest positive-sloped linear correlation with Hg_T among these elements signals the most likely dominant impact of host phase variability in that section of the core. To account for differences in resolution between Hg and XRF data, K_{clr} values were averaged to obtain a K_{clr} value corresponding to the interval covered by each discrete Hg sample (~0.5 cm thickness).

3.5. Mercury accumulation

The total Hg mass accumulation rate (Hg_{AR}) in core BOS04-5B was calculated from:

$$Hg_{AR} = Hg_T\,(DBD \times SR) \qquad \textit{(eqn. 3)}$$

where Hg_{AR} is in mg m^{-2} kyr^{-1}, Hg_T is the total mercury concentration (mg g^{-1}), DBD is the dry bulk density (g m^{-3}), and SR is the sediment accumulation rate (m kyr^{-1}). Values for Hg_{AR} are also

calculated with respect to the median age estimate for each sample. We do not present maximum and minimum Hg_{AR} values here, but note that uncertainties increase with depth due to increasing uncertainties in sedimentation rates calculated based on the BOSMORE7 age model and average ~0.08 cm yr^{-1} (0.02–0.3 cm yr^{-1}).

DBD values were calculated using the formula:

$$DBD = M_{solid}/V_{total} \qquad \textit{(eqn. 4)}$$

where M_{solid} is the mass of dry solid material (g) in each sample, and V_{total} is the volume of each respective sample (0.5 cm^3). To calculate M_{solid}, the proportion of clastic material was multiplied by an assumed grain density value (2.6 g cm^{-3}) representative of a mixture of common sedimentary minerals (e.g. quartz, clay minerals, clastic; typically range of 2.6 to 3 g cm^{-3}) and the total volume. The proportion of clastic material was calculated by first accounting for the proportion of water and organic matter (using loss-on-ignition; McKay (2012) and Shanahan et al. (2013) in each sample and assuming the residual was all clastic material. DBD values generally increase with core depth, reflecting the impact of increasing sediment compaction and dewatering with age (Shanahan et al., 2013). Calculated values of DBD average 1.15 g cm^{-3}, and so are broadly consistent with measurements taken from other African lake sediment successions of similar age (<100 ka), composition (silty clays between 0.6–1.1 g cm^{-3}), and structure (high porosity) (e.g., Cohen et al., 2016; Scholz et al., 2007).

3.6. Statistical analyses

Two statistical analyses were used in order to more quantitatively explore the timing, and expression of signals recorded in the BOS04-5B Hg_T dataset. First was a simple linear Pearson's correlation analysis (**ST6**), from which correlation coefficients (r) were calculated to indicate the direction and strength of the association between Hg (n = 157), and a suite of geochemical proxies also measured in the core. Second was a change point analysis (**ST7**), to determine whether distinct changes in mean values of Hg_T occur within the record using PAST v.4.16 software (Hammer et al., 2001). This software employs a Bayesian Markov chain Monte Carlo (MCMC) approach, which was run on default settings with a total of 1 million MCMC simulations were run for each test and a maximum of ≤10 changepoints. The extent to which similar processes influenced the concentration of Hg_T, TOC, K, and detrital matter were also explored, and correlations were subdivided based on visual examination of the Hg_T records (and supported by changepoint analyses).

4. Results

Core BOS04-5B from Lake Bosumtwi shows distinct fluctuations in total sedimentary Hg concentration (Hg_T) throughout the ~47 m succession. Values range from 10 to 370 ng g^{-1} (median: 58 ng g^{-1}) (**Fig. 2**). The Hg_T curve broadly tracks that of TOC; the latter showing similarly pronounced

418 variability ranging between 0.1 to 23 wt. % (median: 6.5 wt. %) (**Fig. 2**), and peaking between 5.2 and
419 3 m depth. Calculated Hg accumulation rates (Hg_{AR}) do not follow the same pattern as Hg_T and TOC.
420 Ranging between 2.9 and 460 mg m^{-2} kyr^{-1}, calculated values instead broadly track the sedimentation
421 rate curve presented in **Figure 2**. Large peaks in Hg_{AR} are visible between 8 and 6 m depth and then
422 again between 2 and 0 m, and these Hg_{AR} peaks are both coeval with reductions in TOC below ~10
423 wt.%. The lowest Hg_{AR} values are recorded in the lower core section between ~47 and 34 m depth.

424 Changing Hg signals in Lake Bosumtwi correspond to measurable changes in lake sedimentation.
425 From ~47 to 32 m depth, low amplitude, muted variability in both Hg_T and Hg_{AR} corresponds to a
426 homogeneous sequence of silty-clay sized material generally depleted in TOC, S, and high in detrital
427 materials. No clear changes in Hg_T nor Hg_{AR} are visible during AI-1 (34 – 32 m core depth), however,
428 variability in Hg concentration increases immediately following this interval. From ~32 m to the core
429 top, sediments show a progressive increase in Hg_T punctuated by several clear peaks, and more
430 pronounced fluctuations in Hg_{AR} (**Fig. 2**). This shift in Hg behaviour tracks a broad increase in the
431 organic content of the core, reflected by increasing TOC and decreasing clastic material percentages
432 (**Fig. 2**). The clearest expression of this correspondence is seen between 5.2 and 3 m, whereby the
433 highest Hg_T values correspond to the organic-rich sapropel Unit S1.

434 Studying time-resolved changes in lake sediment Hg concentration provides a valuable opportunity to
435 study changes in the pre-industrial Hg cycle, how these changes translate to measurable sedimentary
436 signals, and their links to local and regional-scale environmental variability (Cooke et al., 2020). Two
437 mechanisms emerge as plausible drivers of Hg variability in Lake Bosumtwi (**Fig. 2**). First is organic
438 matter (host) availability, and second is external change in net Hg input to the system.

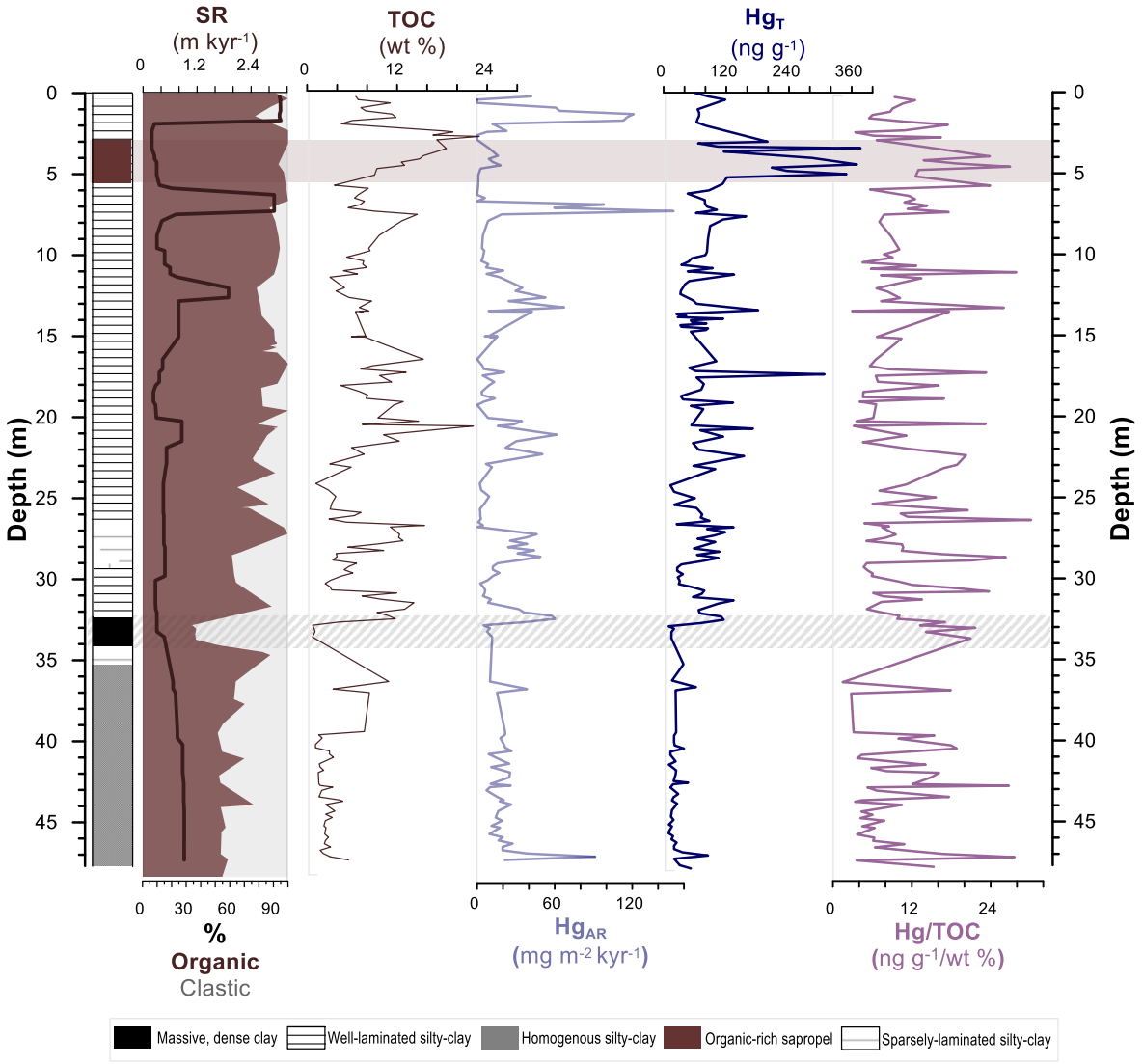

Figure 2: Depth-resolved profiles of total organic carbon (TOC), total Hg (Hg_T) and Hg accumulation rate (Hg_{AR}) profiles obtained for core BOS04-5B from Lake Bosumtwi in this study, relative to key lithofacies and sedimentological data including records of sedimentation rate (SR; *this study*), and the proportion of biogenic to terrigenous material (% organic) within the core (McKay, 2012). A distinct lake low stand referred to as Arid Interval 1 (AI-1) based on seismic profiles and sedimentological data is marked between 33.5 and 32.8 m depth (grey dashed shading; McKay, 2012; Scholz et al., 2007). Limited samples were available between ~39 and 34 m depth (**Fig. SF1**). Sapropel layer Unit S1 is marked between 3–5.5 m depth (brown shading; Russell et al., 2003; Shanahan et al., 2008a; Talbot and Johannessen, 1992). We also present ratios of Hg_T to TOC, following evidence for a positive correlation between the two compounds ($r = 0.64$; $r^2 = 0.42$) (see **section 4.1**).

4.1. Lacustrine host phases of mercury

An overall positive association between Hg_T and TOC ($r = 0.64$; $r^2 = 0.42$) suggests that Hg variability may be associated with organic carbon variability in Lake Bosumtwi. However, it is noteworthy that detrital materials (e.g., K_{clr}) show negative correlations with both TOC ($r = -0.59$; $r^2 = 0.34$) and Hg ($r = -0.57$; $r^2 = 0.32$) so that the Hg-TOC correlation may reflect, in part, a correlation imposed by variable

clay-dilution of both Hg and TOC. Moreover, these correlations are all significant at p <0.001 (unless stated otherwise). The broad statistical link between Hg and TOC is supported by evidence for large Hg_T and Hg_{AR} peaks in core sections containing high TOC concentrations, most markedly in the upper sections (**Fig. 2**), and the relationship between Hg_T and TOC also strengthens following deposition of Al-1 (**Fig. 3b**). However, the highest Hg_T values are not always recorded in the most TOC-enriched sediments, nor are TOC-depleted sediments also depleted in Hg_T (**Fig. 2**). Dilution of Hg by organic matter is unlikely to be the cause (Machado et al., 2016), nor can shift from an organic to detrital-dominated host-phase regime account for these signals, given that intervals characterised by an overall negative Hg and TOC correlation are coeval with similarly negative values for Hg_T and K_{clr} (**Fig. 3, SF4**). More likely is that they reflect changes in net Hg flux to the system, and hence the amount of Hg being supplied to (and sequestered in) Lake Bosumtwi.

A negative overall correlation between Hg_T and K_{clr} is apparent throughout the record ($r = -0.57$; $r^2 = 0.32$; **Fig. 3b, SF4**). Other robust proxies for the proportion of detrital and autochthonous components in biogenic-rich sediments include Fe, Ti, Rb, and Al (**Fig. SF5**) (Grygar et al., 2019). Strong correlations between K_{clr} and these detrital elements confirm this is likely also the case in Lake Bosumtwi (**Fig. 3**), with enrichment of detrital materials in this core reflecting enhanced erosion and sediment transport to the BOS04-5B drill site (McKay, 2012; Shanahan et al., 2012). Moreover, the significant negative correlations between TOC, Hg_T, and all elements associated with detrital components (K_{clr}, Ti_{clr}, Rb_{clr}, and Al_{clr}) (**Fig. 3**) suggest that detrital matter did exert a control on Hg_T. However, instead of increasing Hg, the negative correlation with detrital material suggests that 'Hg-depleted' detrital materials diluted the concentration of both Hg and its suggested host (TOC). Variations in both the detrital and Hg flux may also explain the somewhat counterintuitive decoupling of Hg_T and Hg_{AR} in some intervals, for example, between ~10 and 6 m depth (**Fig. 2**). Dilution-driven alteration of the sedimentary Hg record may be a common feature for depositional systems where supply of Hg is ultimately limited by atmospheric inputs (e.g., Chede et al., 2022).

Strong correlations between Hg_T and Mn_{clr}, and Hg_T and Fe_{clr} (redox sensitive elements) are also absent in BOS04-5B (**Fig. 3**). The majority of the examined record is marked by the presence of laminations, suggesting anoxic conditions dominate throughout (Shanahan et al. 2008). Although this means that redox changes were likely subtle, the coeval presence of siderite has potential implications for Hg through, for example, it's influence on Hg reduction (e.g., Ha et al. 2017). Fe is a major component of siderite, but it is also an important component of the detrital material that washes into Lake Bosumtwi and also potentially other redox-sensitive minerals precipitated in the lake and sediment pore waters (Shanahan 2006; Shanahan et al., 2008; 2009). In this record, we therefore test the relation between Hg_T and Mn peaks. Pronounced Mn enrichments signal periods of (mangano)siderite formation, and this constitutes the clearest indicator of (subtle) pore water redox changes (McKay, 2012; Shanahan et al., 2008). Moreover, siderite specifically may be involved in Hg cycling through its potential to reduce Hg (e.g., Ha et al. 2017). Overall, the lack of evidence for substantial redox changes from ubiquitous laminations and the absence of a strong correlation

482 between Mn and Hg_T suggests that Hg concentrations in Lake Bosumtwi were not appreciably
483 influenced by changes in redox conditions, nor the diagenetic effects signalled by these elements.

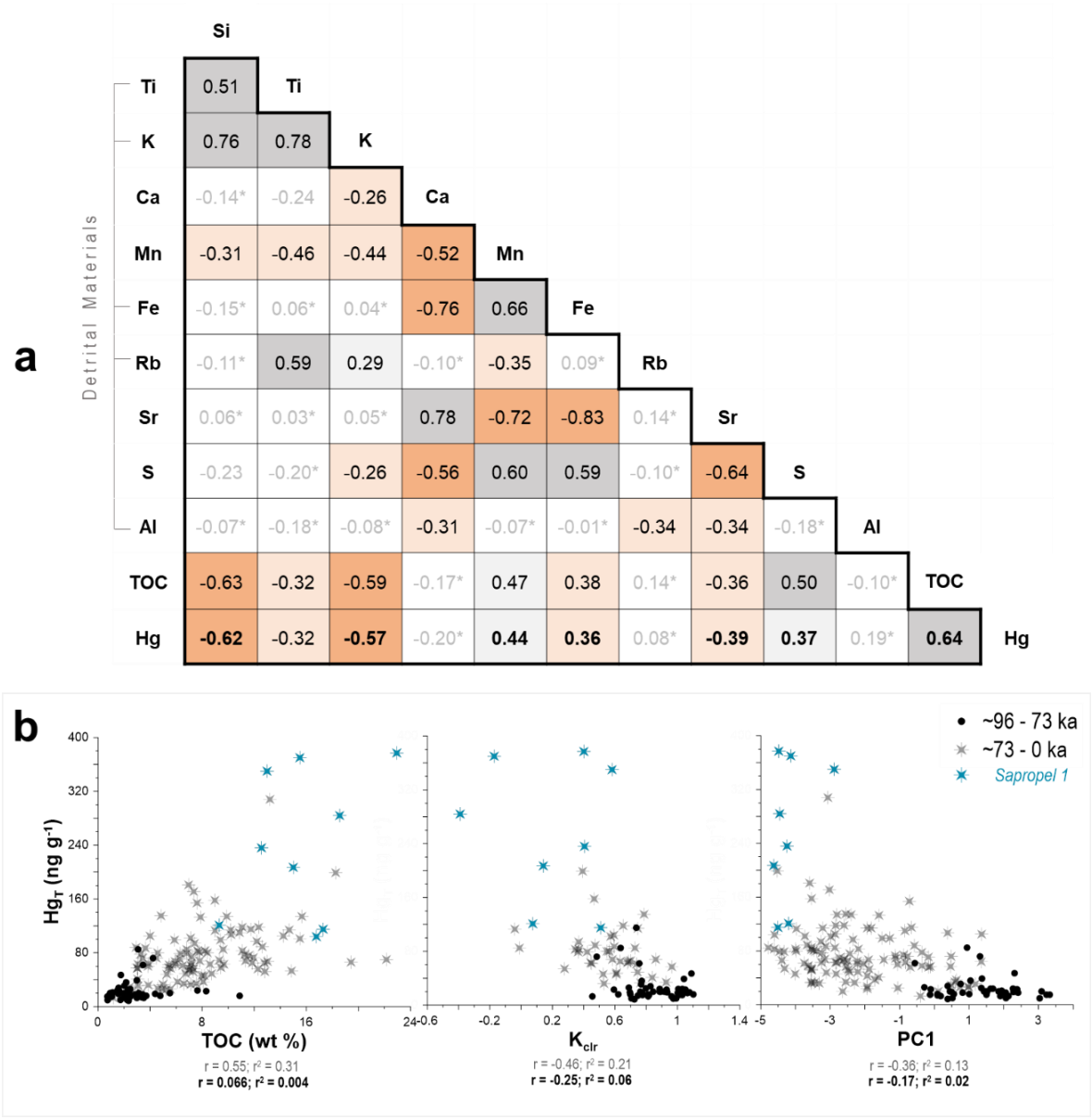

Figure 3: (a) Full-core correlation (Pearson's r) matrix for Hg, total organic carbon (TOC) (this study), and a suite of clr-transformed XRF data measured in BOS04-5B by XRF (McKay, 2012). Sample size (n) was 157 for each analysis, and >50% of the assessed trace element combinations were significant ($p<0.01$). Those combinations that were not are marked with an asterisk (*). Grey shading marks positive correlations (light: >0.25, dark: >0.5), and orange shading marks negative correlations (light: <-0.25, dark: <-0.5). Unshaded boxes mark weak/negligible correlations (between 0 and 0.25, and 0 and -0.25), with values greyed-out for clarity. All remaining values are presented with black text, with those in this range related to Hg in the boldest type. **(b)** Comparison of relationships in Lake Bosumtwi between ~96 and 73 ka (black circles), and between ~73 and 0 ka (stars). Relationships presented here are between Hg_T, total organic carbon (TOC), detrital minerals (estimated by potassium (K)) concentrations; McKay (2012), and principal component 1 (PC1) of the BOS04-5B XRF data, in which 39% of total variance is strongly associated with terrigenous elements (McKay, 2012). R (r) and r-squared (r^2) values for each interval are also given, and Student's t-testing showed that the

significance of all correlations were significant at $p<0.01$ Stars marked in teal correspond to deposition of sapropel unit 1 (S1) in BOS04-5B.

5. Discussion

5.1. Environmental drivers

Time resolved Hg_T and Hg_{AR} profiles generated from the sediments of Lake Bosumtwi show two broad periods of differing Hg behaviour: (1) ~96 – 73 ka (low Hg_T and Hg_{AR}) and (2) ~73 – 0 ka (moderate/high Hg_T, and large fluctuations in Hg_T and Hg_{AR}) (**Fig. 4**). Each corresponds to different lake level evolution trends with broadly decreasing lake level between ~96 and 73 ka (although with a substantial rise between 95 and 80 ka), and rising from ~73 to 0 ka (**Fig. 4**). Lake Bosumtwi's hydrology is controlled by a balance between direct precipitation and runoff with water removal limited almost entirely to evaporation; exceptions being rare transient overspilling events (Turner et al., 1996). Taking this unique hydrology into account, our discussion below explores how different environmental processes relate to changes in Hg behaviour during these two distinct intervals, and how the significance of these processes may have changed through time.

5.1.1. Arid conditions (~96 to 73 ka)

Both Hg_T and Hg_{AR} show muted variability between ~96 and 73 ka (**Fig. 4**). The presence of more clastic-rich/organic-depleted sediment (**Fig. 4**), and reductions in tree pollen are both typical of a savannah-dominant, more open landscape (**Fig. 4)**, and so suggest generally arid conditions within the lake and its catchment prior to ~73 ka. These conditions would favour pronounced reductions in lake level (McKay, 2012; Miller et al., 2016; Scholz et al., 2007), and are consistent with a 24 – 38% reduction in local rainfall as estimated by water balance modelling) (Shanahan et al., 2008b). Reductions in lake level could facilitate an increase in water column vertical mixing, ventilation of bottom waters, more efficient breakdown of organic matter, and simultaneous sediment dilution by a sudden increase in eroded material fluxes (McKay, 2012; Scholz et al., 2007; Shanahan et al., 2012) – all could lead to a reduction in organic matter (host-phase) concentration. Indeed, several meromictic lakes have shown reduced organic matter content as a function of better ventilation and lower productivity during 'shallow' conditions (Katsev et al., 2010; Schultze et al., 2017), and new evidence suggests that changes in organic matter oxidation may produce comparably distinct changes in Hg sequestration (Tisserand et al., 2022).

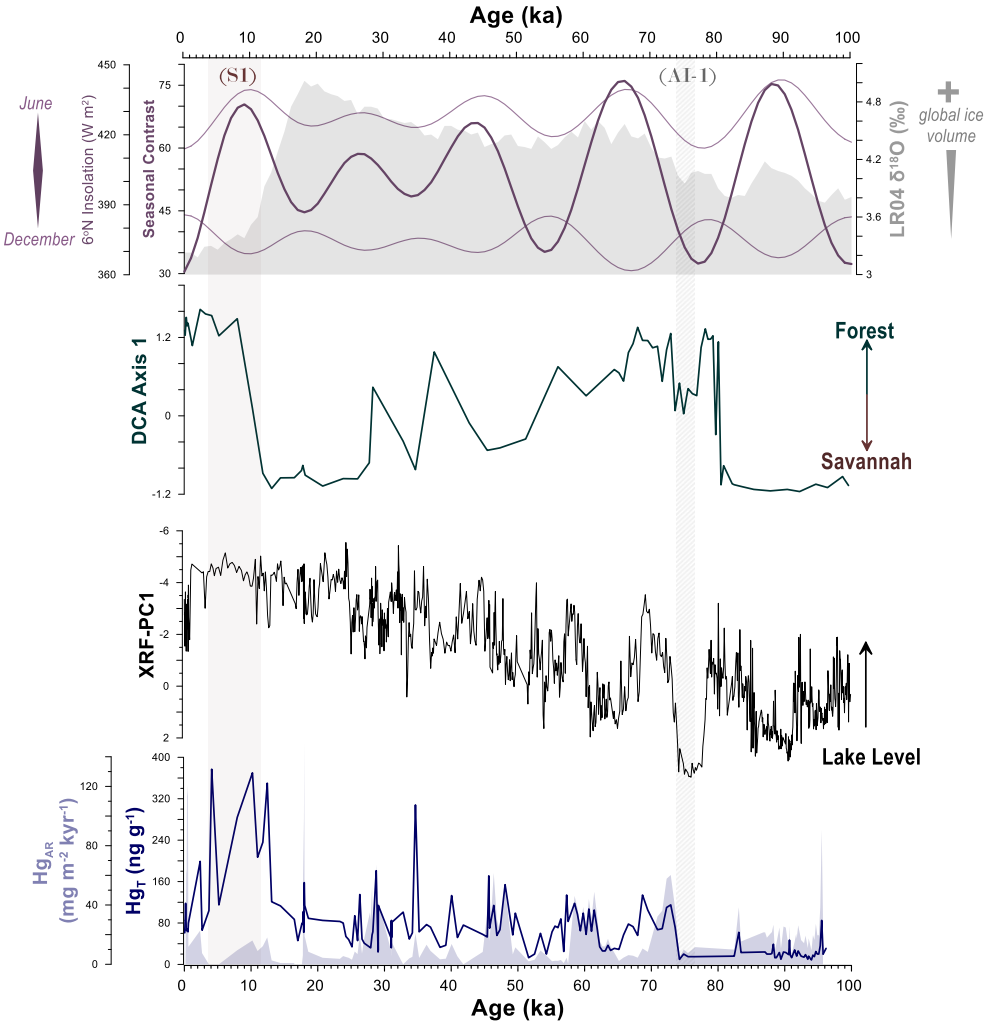

Figure 4: Comparison of key proxy datasets. Included are (from bottom to top), total mercury (Hg_T) and mercury accumulation rate (Hg_{AR}) for Lake Bosumtwi from this study (see **section 5.1**), the first principal component (PC1) of the BOS04-5B XRF data (39% of total variance, interpreted as an indicator of lake level changes; McKay, 2012), forest (woody) taxa abundance (presented as DCA Axis 1; Gosling et al., 2022a; Miller et al., 2016), and insolation at 6ºN (location of Lake Bosumtwi) in June (summer) and December (winter) calculated following the astronomical solution presented by Laskar et al. (2004) (accessed via. https://vo.imcce.fr/insola/earth/online/earth/online/index.php), and used to calculate seasonal insolation contrast. Also shown is a record of benthic foraminiferal calcite $\delta^{18}O$ (‰) derived from the LR04 global stack) as a proxy for ice volume, with cold glacial stages defined by high $\delta^{18}O$ ratios (Lisiecki and Raymo, 2005a). Proxy data are all presented on the BOSMORE7 chronology. Unit AI-1 is marked between 33.5 and 32.8 m depth (grey shading; Brooks et al., 2005; Scholz et al., 2007), and sapropel layer Unit S1 is marked between 3–5.5 m depth (brown shading; Shanahan et al., 2012, 2006).

The absence of a clear change in Hg_{AR} between ~96 and 73 ka might also reflect changes in the balances of Hg cycling in the lake. Lake Bosumtwi is a hydrologically closed system that receives >80% of its water from rainfall directly on the surface, meaning its hydrology and sedimentation regime is extremely sensitive to variability in precipitation and precipitation-evaporation balance (Shanahan et al., 2007; Turner et al., 1996). Thus, low Hg_T and Hg_{AR} values may reflect a reduction in wet deposition of atmospheric Hg at the Lake Bosumtwi site by precipitation, while Hg evasion back to

the atmosphere remains high due to evaporation in the consistently warm, tropical temperatures (Schneider et al., 2023). Depletion of sedimentary Hg during drier climate intervals are documented in several other late Quaternary-age records, where they are interpreted as signs of a net reduction in Hg input relative to loss/evasion (e.g., Hermanns and Biester, 2013; Pompeani et al., 2018; Schneider et al., 2020; Schütze et al., 2021, 2018).

Desiccation of Lake Bosumtwi between ~75 and 73 ka (AI-1) corresponds to evidence for severe depletion of organic matter, and enrichment of detrital materials within the sediments (**Fig. 2**). Although a detailed characterization of local soil and bedrock Hg contents is currently lacking for Lake Bosumtwi, these changes in sediment composition (lower TOC, higher K_{clr}) and low overall sedimentation rates are unaccompanied by coeval changes in Hg_{AR} (**Fig. 2**). In certain cases, one would typically expect that the near-complete desiccation of a steep-sided lake would 'focus' trace metals (including Hg) at the central coring site, particularly during lake recessions following erosion of exposures around the crater rim (Blais and Kalff, 1995; Engstrom and Rose, 2013). However, evidence for low Hg burial both prior to and during AI-1 in Lake Bosumtwi suggests that over multiple millennia, changes in Hg supply to the BOS04-5B drill site were predominantly driven by atmospheric inputs, with minimal contribution from catchment-sourced materials.

5.1.2. Humid conditions (~73 to 0 ka)

The magnitude and frequency of variability in Hg_T visibly increases at ~73 (±5) ka (**Fig. 4**). The quantitative significance of this shift is supported by changepoint analysis of the BOS04-5B dataset, which demonstrates a clear and step-wise shift in mean Hg_T values between ~75 and 73 ka (**Fig. SF3**). It also occurs in conjunction with an increase in the lake's water level (**Fig. 4b**), which is corroborated by a statistically significant relationship between PC1 (lake level indicator; McKay, 2012), and Hg_T in our record (**Fig. 3b** - $r = -0.36$; $r^2 = 0.13$). Furthermore, changing sedimentary TOC, terrigenous material, and pollen concentrations all corroborate a broad increase in local moisture availability, temperature, and humidity following deposition of the AI-1 unit (**Fig. 4**): a signal that coincides with the transition into the warmer Holocene interglacial, marked by reduced global ice volume and increased sea surface temperatures in the North Atlantic (McKay, 2012; Scholz et al., 2007; Shanahan et al., 2008b). Our data also shows a simultaneous increase in Hg_T, and a decrease in detrital material concentrations following ~73 ka (**Fig. 4**), suggesting that Hg supply temporarily exceeded the diluting effects of clastic materials following lake level rise.

Lake deepening generally increases water column stratification, limiting the effects of vertical transport processes such as turbulent energy generated by surface winds and currents (Gulati et al., 2017). Deeper, more anoxic conditions are also typically associated with more effective organic carbon burial (Gulati et al., 2017; Schultze et al., 2017), coupled with more distinct formation of distinct laminations (Zolitschka et al., 2015) and precipitation of authigenic carbonates such as siderites (Swart, 2015). Given that elevated Hg_T and Hg_{AR} correlate most closely with TOC enrichment in Lake Bosumtwi following ~73 ka (**Fig. 3b**), this could suggest that Hg drawdown was

556 moderated by an increase in organic matter availability and preservation, as an indirect function of
557 bottom water deoxygenation. Evidence for an inverse relationship between sedimentary Hg
558 concentration and hypolimnion oxygen content has been identified in a number of meromictic lake
559 systems across the world (e.g., Schultze et al., 2017; Tisserand et al., 2022), and provides further
560 support for our interpretation.

561 Geochemical and sedimentological evidence suggests near-permanent oxygen depletion in Lake
562 Bosumtwi following ~73 ka, which likely contributed to formation of a very organic-rich sapropel
563 formation between 12.4 and 3.7 ka. This unit contains clear Hg_T enrichments relative to the rest of the
564 core (**Figs. 2, 4a, SF3**), is extremely rich in organic matter (~15-20%), and contains a high
565 concentration of blue-green algae *Anabaena* deposits (Russell et al., 2003). Sapropelic layers have
566 emerged as key sites of Hg enrichment from a suite of marine and lacustrine-based studies,
567 suggesting this may be due to changes in productivity, sediment oxygenation, and diagenetic
568 processes (e.g., Frieling et al., 2023; Gehrke et al., 2009; Jeon et al., 2020). Scavenging of Hg from
569 the water column by algae is also recognised as an important driver of Hg export to lacustrine
570 sediments; particularly in systems where primary productivity, organic matter production, and burial
571 capacity is high (Biester et al., 2018; Schütze et al., 2021; Outridge et al. 2007). These conditions are
572 met in Lake Bosumtwi following ~73 ka, meaning the observed changes in sedimentary Hg_T could be
573 linked to elevated rates of scavenging, as a function of enhanced primary productivity.

574 In closed-basin lakes where fluxes of organic material from the catchment (e.g., soils and vegetation)
575 are minimal, measurable changes in sedimentary Hg concentration would require a simultaneous
576 increase in Hg fluxes to the system in order to counterbalance Hg depletion by scavenging,
577 methylation, or evasion back to the atmosphere (e.g., Bravo et al., 2017; Hermanns et al., 2013;
578 Outridge et al., 2007; Schütze et al., 2021). For Lake Bosumtwi these direct inputs may have come
579 from precipitation, and/or from increased flux of charcoal and associated release of Hg from
580 vegetation during wildfires into the lake following local wildfire events; the latter documented by
581 variations in the micro charcoal concentration of BOS04-5B (Gosling et al., 2021; Miller et al., 2016;
582 Miller and Gosling, 2014).

583 Data from Lake Bosumtwi suggests an increase in local precipitation following ~73 ka. Model and
584 proxy-based data show that the precipitation-evaporation balance is directly coupled to lake level in
585 this system, such that lake deepening occurs as a function of more rainfall (Shanahan et al., 2008b).
586 Proxy data generated from the BOS04-5B core suggest that progressively wetter conditions affected
587 the catchment following ~73 ka (e.g., Gosling et al., 2022a; Shanahan et al., 2008b). Paleoclimate
588 records based on the sediments of lakes Malawi (Tanzania), Bambili (Cameroon), Tanganyika
589 (Tanzania/Democratic Republic of the Congo), Chew Bahir (Ethiopia) and Chala (Tanzania) (e.g.,
590 Cohen et al., 2007; Foerster et al., 2022; Lézine et al., 2019; Scholz et al., 2007), and marine
591 sediment core material from the West African margin (**Figs. 1, 5**) (e.g., Kinsley et al., 2022;
592 Skonieczny et al., 2019) also pertain to a distinct regional-scale shift in hydro climate across tropical
593 sub-Saharan Africa at this point in time (**Fig. 5**). Specifically, a shift characterized by a distinct
594 moisture gradient favouring wetter conditions in the west of the continent relative to the east, which

was further amplified during the last glacial termination (e.g., Baxter et al., 2023; Gosling et al., 2022a; Lupien et al., 2023). Therefore, the coeval increase in the frequency and amplitude of Hg enrichments in Lake Bosumtwi, and associated rises in lake level, could indirectly reflect pronounced shifts in hydroclimate across tropical sub-Saharan Africa.

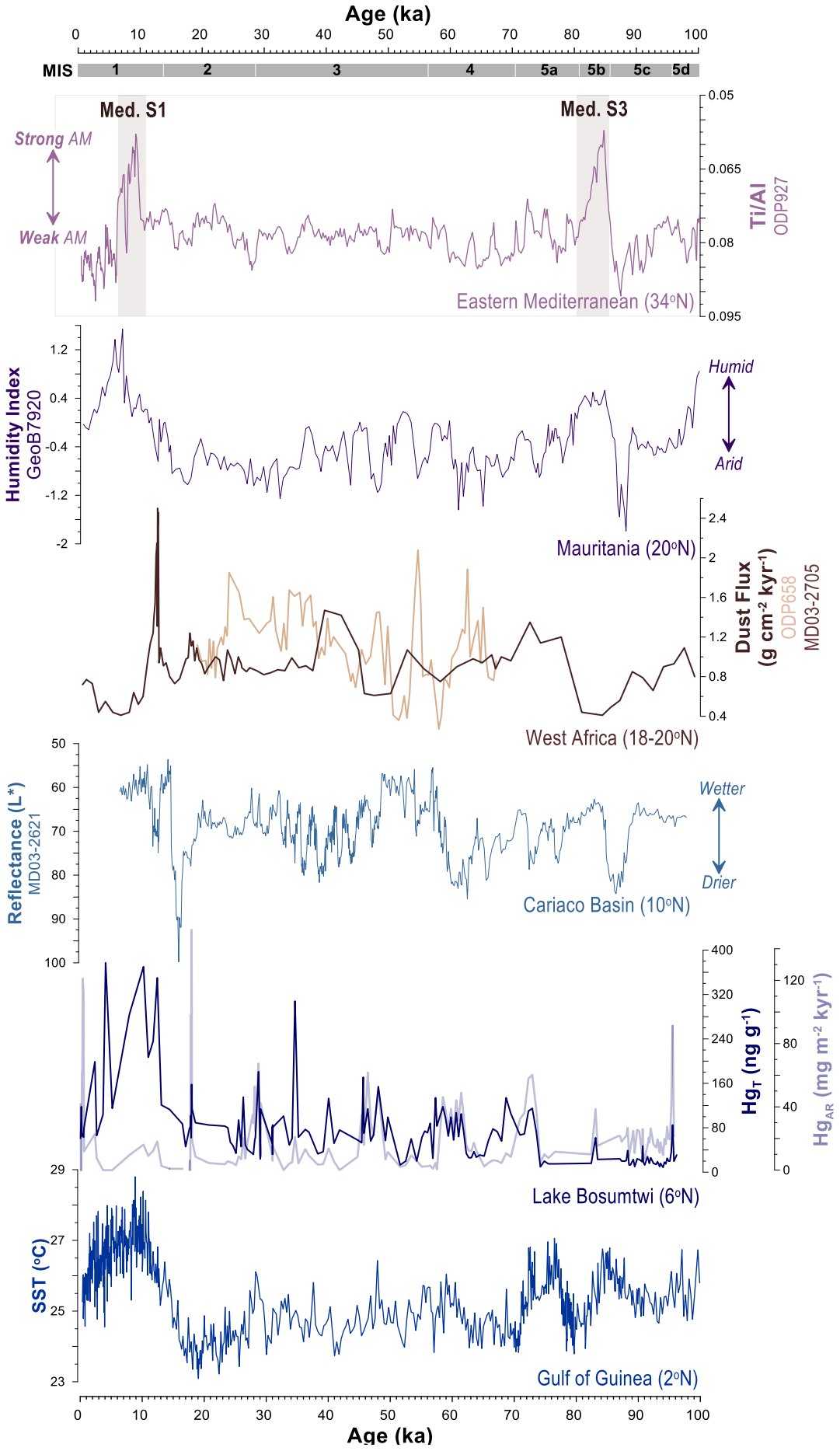
Age (ka)
0
10
20
30
40
50
60
70
80
90
100
MIS
1
2
3
4
5a
5b
5c
5d
Med. S1
Med. S3
Strong AM
Weak AM
Ti/Al
ODP927
Eastern Mediterranean (34°N)
0.05
0.065
0.08
0.095
Humidity Index
GeoB7920
Humid
Arid
1.2
0.4
-0.4
-1.2
-2
Mauritania (20°N)
Dust Flux
(g cm-2 kyr-1)
ODP658
MD03-2705
2.4
2
1.6
1.2
0.8
0.4
West Africa (18-20°N)
Reflectance (L*)
MD03-2621
Wetter
Drier
50
60
70
80
90
100
Cariaco Basin (10°N)
HgT (ng g-1)
HgAR (mg m-2 kyr-1)
400
320
240
160
80
0
120
80
40
0
29
Lake Bosumtwi (6°N)
SST (°C)
27
25
23
Gulf of Guinea (2°N)
Age (ka)

Figure 5: Records of total mercury (Hg_T) and mercury accumulation rate (Hg_{AR}) for Lake Bosumtwi generated by this study, compared with key paleoclimate records presented in order of latitude (physical locations shown in **Figure 1**), and known to be influenced by the WAM: sea-surface temperature (SST) reconstructed in core MD03-2707 from the Gulf of Guinea (Weldeab et al., 2007), sediment total reflectance (L*) in marine core MD03-2621 from the Cariaco Basin, Venezuela, as a proxy for hydrological conditions anticipated in light of ITCZ oscillations over West Africa (Deplazes et al., 2013), dust fluxes recorded in cores ODP658 (Cap Blanc; Kinsley et al., 2022) and MD03-2705 (; Skonieczny et al., 2019), and a continental humidity index of core GeoB7920-2 (Mauritanian seamount; Tjallingii et al., 2008) – all from offshore Mauritania. Finally, Ti/Al recorded in core ODP 927 from the Eastern Mediterranean as a record of riverine (low Ti/Al) versus aeolian (high Ti/Al) North African inputs to the Mediterranean basin, and thus African monsoon intensity (Grant et al., 2022, 2017). Mediterranean sapropels one (Med. S1) and three (Med. S3) are marked by light brown bars (Grant et al., 2016). Light grey bars mark marine isotope stages (MIS) defined by the LR04 benthic marine isotope stack (Lisiecki and Raymo, 2005b).

Volcanic and wildfire activity are both linked to the Hg cycle. Although Lake Bosumtwi is located in close proximity to several highly productive volcanic regions, the resolution of BOS04-5B precludes our ability to examine Hg emissions with respect to single eruption events (**Fig. SF7**), and eruption record incompleteness coupled with time-transgressive changes in the global atmospheric Hg burden both complicate the ability to unambiguously correlate enhanced volcanic emissions to greater Hg deposition (**Fig. SF7**). Hydroclimate was also a key driver of changes in fire activity in tropical sub-Saharan Africa during the late Pleistocene (Moore et al. 2022). However, although wetter climatic conditions may be broadly associated with heightened fire activity due to associated increases in terrestrial biomass, recent work has shown that discrete changes in precipitation can elicit notably different fire responses between sites (e.g., Gosling et al., 2021; Karp et al., 2023). The influence of biomass burning on the Hg record presented here appears similarly complex; despite being a well-constrained factor in the Bosumtwi catchment, and evidence that wildfires are also a significant source of Hg, accounting for ~13% of natural Hg (re-)emissions to the modern atmosphere (Francisco López et al., 2022). Given that no clear relation is visible between Hg_T, Hg_{AR}, and two discrete macro- (Kiely, 2023) and micro- (Miller et al., 2016) charcoal profiles generated from the BOS04-5B core, we suggest that the effects of Hg emitted during wildfires also did not leave a clear imprint on Hg variability in this record (**Fig. SF8**).

6. Synthesis and conclusions

This study combines new sedimentary Hg data from Lake Bosumtwi, Ghana, with proxy data from archives across the African continent to explore whether hydroclimate has exerted a measurable effect on regional Hg cycling over the past ~96-kyr. The resolution of the BOS04-5B record (~0.6 kyr per sample) precludes a detailed assessment of more recent (<0.2-kyr), anthropogenic-driven changes in local Hg cycling. However, this record is well suited for a broader exploration of patterns and drivers of variability in sedimentary Hg concentrations in Lake Bosumtwi during the late

Pleistocene. Combining our results with existing data reveals two possible drivers of variability in Hg_T and Hg_{AR} in Lake Bosumtwi on these timescales: organic matter (host) availability, and local-scale changes in Hg input to the lake by precipitation (**Fig. 4**). Both are intrinsically coupled to the local hydroclimate by their link to the lake level, with higher lake levels typically corresponding to wetter conditions in the catchment, and deposition of more organic-rich sediments. **Figure 6** illustrates how selected environmental processes, under different environmental conditions, may have interacted with these two drivers to control Hg burial in Lake Bosumtwi between ~96 and 0 ka. Considered together, the evidence summarised in panels **(1), (2),** and **(2a)** all suggest that rates of Hg drawdown in Lake Bosumtwi, and indeed the signals retained in the sediment record, reflect changes in net Hg supply from the atmosphere.

Between ~96 and 73 ka (**Fig. 6, panel (1)**), generally arid conditions shifted the lake into a negative water balance. Not only could this have reduced the net flux of Hg to the lake by wet deposition (precipitation), but a negative water balance would also limit internal primary productivity and preservation, and so render less organic material available to sequester any Hg present in the system. Secondary dilution of Hg by detrital materials could have also lowered sedimentary Hg concentrations, with elevated delivery of terrigenous matter to the BOS04 site driven by exposure of the steep-sided crater walls during lake level lowering, and heightened soil instability due to widespread recession of catchment vegetation. All would persist (if not strengthen) during AI-1, and so could explain the lack of any measurable changes in Hg_T and Hg_{AR} during this time.

Following an extended period of aridity, net supply of Hg to the basin would be increased by precipitation following ~73 ka. This would simultaneously cause the lake to become deeper and more stratified (**Fig. 6, panel (2)**). As the bottom waters became more oxygen-depleted, more effective organic matter burial would simultaneously enhance Hg drawdown compared to detrital mineral supply; with higher lake levels, vegetation growth, and soil stabilization preventing exposure and erosion of the crater walls and soils surrounding the lake. Hence, this abrupt shift to humid (net-positive precipitation-evaporation balance) conditions in the Bosumtwi catchment could plausibly have driven an increase in sedimentary Hg concentrations and accumulation, by eliciting a pronounced rise in lake level as well as increasing the atmospheric Hg flux.

The processes described in panel (2) would be amplified further between ~15 and 4 ka (**Fig. 6, panel 2a**). Corresponding to Bosumtwi sapropel unit 1, this unit marks a distinct humid period characterised by anomalously high rainfall, and documented by proxy records across tropical sub-Saharan Africa (Shanahan et al., 2015). For a closed lake system such as Lake Bosumtwi, these wetter conditions would drive a sharp increase in lake depth, stratification, and scavenging in the water column – all could favour heightened Hg drawdown to the sediment. 'Flattening' of the Hg-TOC relationship during this interval also suggests that the Hg supply was (far) exceeded by the organic matter availability (**Fig. 3a**), and so elevated Hg supply by precipitation could explain why Hg_T and Hg_{AR} values are so unusually high (**Fig. 4a, 5**).

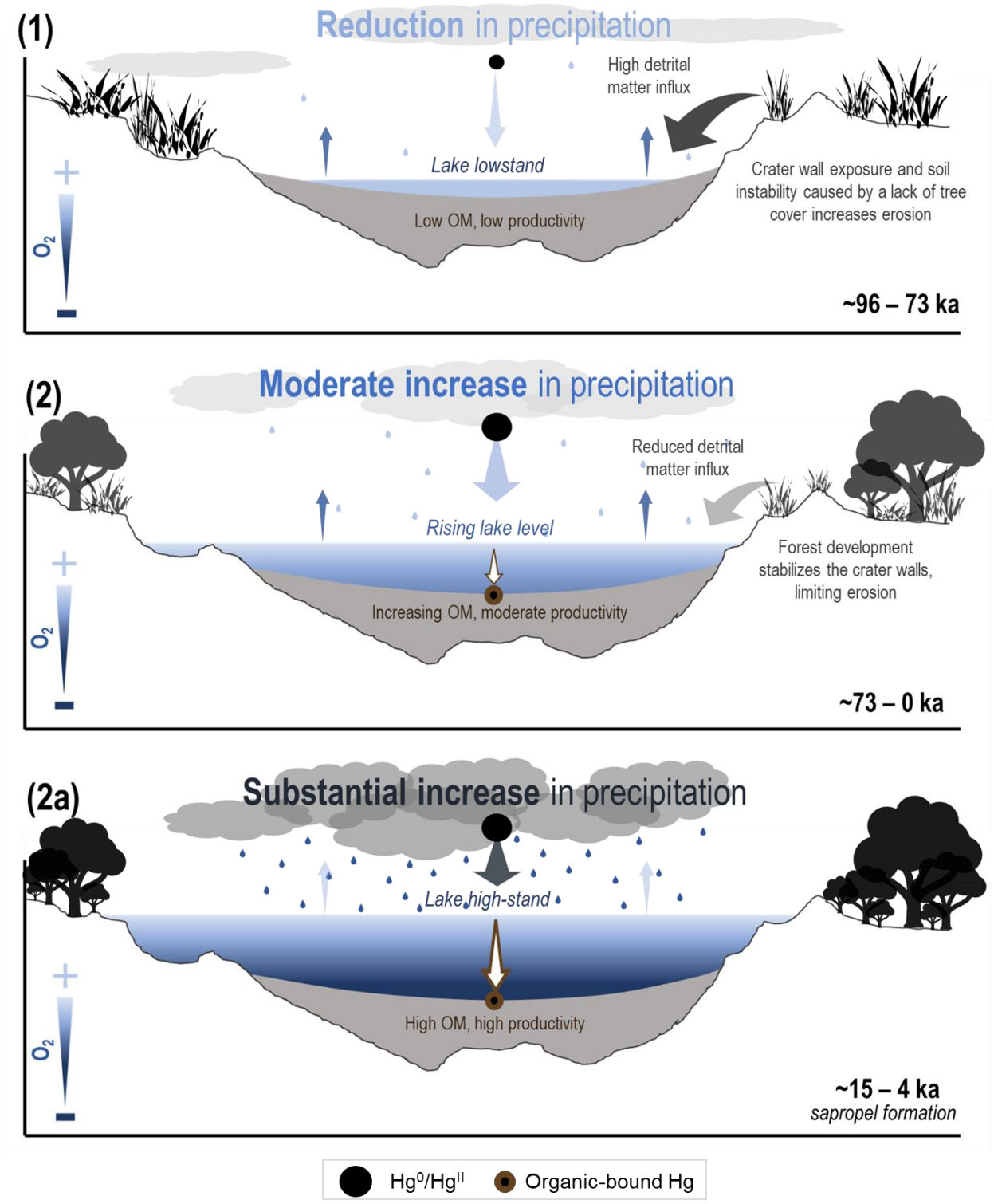

Figure 6: Schematic model depicting the processes that may control Hg flux, accumulation, and burial in Lake Bosumtwi under **(1)** arid (~93 – 73 ka), and **(2)** humid (~73 – 0 ka), environmental conditions. Panel **(2a)** depicts the very humid conditions that would be conducive to sapropel formation, such as those known to have occurred during the African Humid Period (~15 – 4 ka). Taken together, Hg fluxes increase during wet periods due to higher wet deposition directly to the lake relative to evasion, and/or by enhanced mobilization and transport of Hg from the

catchment. Hg sequestration can also be enhanced by OM-scavenging in the water column, and increased lake stratification (anoxia at lake floor). The opposite occurs during dry intervals.

Future research should seek better constraints on how basin-specific variations in sediment composition, lake structure, and water balance may influence how sedimentary Hg signals are preserved and interpreted. This is because all could produce diverse, and perhaps contrasting, results between lake systems. For example, results from Lake Bosumtwi suggest that lakes with smaller watersheds, simple morphology, and minimal hydrological connectivity to the catchment could be suitable targets to study catchment and intra-lake depositional processes over multiple millennia. However, there are currently too few records covering these timescales to say this with certainty, and not all closed lakes record measurable changes in Hg composition corresponding to changes in local hydroclimate (Lent and Alexander, 1996; Pompeani et al., 2018). Organic matter/host phase availability also appears to represent just one of several possible processes governing Hg burial in lacustrine systems, given these systems are more readily affected by short-term changes in erosion, nutrients, water balance, and catchment hydrology (Paine et al., 2024; Schütze et al., 2021).

Lake Bosumtwi is a small, morphologically simple lake. However, the complexity shown by its sedimentary Hg record suggests that identical stratigraphic signals are unlikely to be recorded in separate lakes, even if they are dominated by one common process, mechanism, and/or structure. Exploring the importance of hydroclimate for Hg cycling relative to different catchment to lake area ratios, hydrology (e.g., endorheic (closed) versus exoreic (open)), and/or catchment structures (e.g., forest versus savannah) would undoubtedly help to better resolve processes acting on single lacustrine and terrestrial successions, but also identify the systems that may more sensitively record major changes in Hg cycling. Provided the hydrological component of the Hg cycle can be isolated, better characterization of the processes impacting lacustrine Hg cycling could also allow this element to be used as a proxy for hydroclimatic change in terrestrial archives. For example, measurement of sedimentary Hg isotopes in low-latitude and/or closed lakes could help quantify the contribution of Hg to the sediment from precipitation or dry deposition, shedding new light on key biogeochemical reaction pathways, processes (e.g., mass-independent fractionation (MIF)), and responses to changing local hydrology across a range of timescales (e.g., Blum et al., 2014; Gao et al., 2023; Yin et al., 2024).

This study provides new and valuable evidence for long-term interactions between terrestrial Hg cycling and hydroclimate, and demonstrates that hydroclimate may be a key driver of Hg cycling in tropical lakes over millennial-timescales. The sparse number of continuous, pre-industrial Hg records currently available for sub-Saharan Africa have historically limited the ability to understand if, or how, hydroclimate may drive long-term (>10^2-year) variability in the Hg cycle (Schneider et al., 2023), and subsequently how this relationship is represented in local and global ecosystem models (Cooke et al., 2020; Obrist et al., 2018). Although this knowledge gap cannot be satisfied by a single record, study of Lake Bosumtwi reinforces the value of these records for better characterization of the Hg behaviour likely to be associated with projected future, monsoon-driven, hydroclimate variability (Chang et al.,

2022). In time, this could translate to better understanding of how the tropical Hg cycle may respond to future, global-scale changes (Gustin et al., 2020; Schneider et al., 2023).

Competing Interests

The contact author has declared that none of the authors has any competing interests.

Acknowledgements

ARP, IMF, JF, and TAM acknowledge funding from European Research Council Consolidator Grant V-ECHO (ERC-2018-COG-8187 17-V-ECHO). ARP thanks Christopher Scholz for provision of sediment data, alongside James Bryson, Alex Dickson, Erdem Idiz, Francesco Pausata, Matt Jones, and Victoria Smith for insightful discussions at various stages of manuscript preparation. Thanks also go to Stephen Wyatt (University of Oxford) for analytical assistance throughout the study. All authors thank members of the International Continental Scientific Drilling Program Lake Bosumtwi Drilling Project: for their efforts in extracting and producing the sediment succession, and making the data available for scientific use.

References

Åkerblom, S., Bishop, K., Björn, E., Lambertsson, L., Eriksson, T., Nilsson, M.B., 2013. Significant interaction effects from sulfate deposition and climate on sulfur concentrations constitute major controls on methylmercury production in peatlands. Geochimica et Cosmochimica Acta 102, 1–11. https://doi.org/10.1016/j.gca.2012.10.025

Amos, H.M., Sonke, J.E., Obrist, D., Robins, N., Hagan, N., Horowitz, H.M., Mason, R.P., Witt, M., Hedgecock, I.M., Corbitt, E.S., Sunderland, E.M., 2015. Observational and modeling constraints on global anthropogenic enrichment of mercury. Environmental Science and Technology 49, 4036–4047. https://doi.org/10.1021/es5058665

Armenteros, I., 2010. Diagenesis of Carbonates in Continental Settings, in: Developments in Sedimentology. Elsevier, pp. 61–151. https://doi.org/10.1016/S0070-4571(09)06202-5

Armstrong, E., Tallavaara, M., Hopcroft, P.O., Valdes, P.J., 2023. North African humid periods over the past 800,000 years. Nat Commun 14, 5549. https://doi.org/10.1038/s41467-023-41219-4

Baxter, A.J., Verschuren, D., Peterse, F., Miralles, D.G., Martin-Jones, C.M., Maitituerdi, A., Van Der Meeren, T., Van Daele, M., Lane, C.S., Haug, G.H., Olago, D.O., Sinninghe Damsté, J.S., 2023. Reversed Holocene temperature–moisture relationship in the Horn of Africa. Nature 620, 336–343. https://doi.org/10.1038/s41586-023-06272-5

Benoit, J.M., Gilmour, C.C., Mason, R.P., Heyes, A., 1999. Sulfide controls on mercury speciation and bioavailability to methylating bacteria in sediment pore waterA. Environmental Science and Technology 33, 1780. https://doi.org/10.1021/es992007q

Bertrand, S., Tjallingii, R., Kylander, M.E., Wilhelm, B., Roberts, S.J., Arnaud, F., Brown, E., Bindler, R., 2024. Inorganic geochemistry of lake sediments: A review of analytical techniques and guidelines for data interpretation. Earth-Science Reviews 249, 104639. https://doi.org/10.1016/j.earscirev.2023.104639

Biester, H., Pérez-Rodríguez, M., Gilfedder, B.-S., Martínez Cortizas, A., Hermanns, Y.-M., 2018. Solar irradiance and primary productivity controlled mercury accumulation in sediments of a remote lake in the Southern Hemisphere during the past 4000 years: Primary productivity and mercury accumulation. Limnol. Oceanogr. 63, 540–549. https://doi.org/10.1002/lno.10647

Bin, C., Xiaoru, W., Lee, F.S.C., 2001. Pyrolysis coupled with atomic absorption spectrometry for the determination of mercury in Chinese medicinal materials. Analytica Chimica Acta 447, 161–169. https://doi.org/10.1016/S0003-2670(01)01218-1

Bishop, K., Shanley, J.B., Riscassi, A., de Wit, H.A., Eklöf, K., Meng, B., Mitchell, C., Osterwalder, S., Schuster, P.F., Webster, J., Zhu, W., 2020. Recent advances in understanding and measurement of mercury in the environment: Terrestrial Hg cycling. Science of the Total Environment 721. https://doi.org/10.1016/j.scitotenv.2020.137647

Blais, J.M., Kalff, J., 1995. The influence of lake morphometry on sediment focusing. Limnol. Oceanogr. 40, 582–588. https://doi.org/10.4319/lo.1995.40.3.0582
Blum, J.D., Sherman, L.S., Johnson, M.W., 2014. Mercury Isotopes in Earth and Environmental Sciences. Annu. Rev. Earth Planet. Sci. 42, 249–269. https://doi.org/10.1146/annurev-earth-050212-124107
Boamah, D., Koeberl, C., 2007. The Lake Bosumtwi impact structure in Ghana: A brief environmental assessment and discussion of ecotourism potential. Meteoritics and Planetary Science 42, 561–567. https://doi.org/10.1111/j.1945-5100.2007.tb01061.x
Bradley, R.S., Diaz, H.F., 2021. Late Quaternary Abrupt Climate Change in the Tropics and Sub-Tropics: The Continental Signal of Tropical Hydroclimatic Events (THEs). Reviews of Geophysics 59, e2020RG000732. https://doi.org/10.1029/2020RG000732
Branfireun, B.A., Cosio, C., Poulain, A.J., Riise, G., Bravo, A.G., 2020. Mercury cycling in freshwater systems - An updated conceptual model. Science of the Total Environment 745. https://doi.org/10.1016/j.scitotenv.2020.140906
Bravo, A.G., Bouchet, S., Tolu, J., Björn, E., Mateos-Rivera, A., Bertilsson, S., 2017. Molecular composition of organic matter controls methylmercury formation in boreal lakes. Nat Commun 8, 14255. https://doi.org/10.1038/ncomms14255
Brodie, C.R., Leng, M.J., Casford, J.S.L., Kendrick, C.P., Lloyd, J.M., Yongqiang, Z., Bird, M.I., 2011. Evidence for bias in C and N concentrations and δ13C composition of terrestrial and aquatic organic materials due to pre-analysis acid preparation methods. Chemical Geology 282, 67–83. https://doi.org/10.1016/j.chemgeo.2011.01.007
Brooks, K., Scholz, C.A., King, J.W., Peck, J., Overpeck, J.T., Russell, J.M., Amoako, P.Y.O., 2005. Late-Quaternary lowstands of lake Bosumtwi, Ghana: Evidence from high-resolution seismic-reflection and sediment-core data. Palaeogeography, Palaeoclimatology, Palaeoecology 216, 235–249. https://doi.org/10.1016/j.palaeo.2004.10.005
Brumsack, H.J., 2006. The trace metal content of recent organic carbon-rich sediments: Implications for Cretaceous black shale formation. Palaeogeography, Palaeoclimatology, Palaeoecology 232, 344–361. https://doi.org/10.1016/j.palaeo.2005.05.011
Chang, M., Liu, B., Wang, B., Martinez-Villalobos, C., Ren, G., Zhou, T., 2022. Understanding Future Increases in Precipitation Extremes in Global Land Monsoon Regions. Journal of Climate 35, 1839–1851. https://doi.org/10.1175/JCLI-D-21-0409.1
Chede, B.S., Venancio, I.M., Figueiredo, T.S., Albuquerque, A.L.S., Silva-Filho, E.V., 2022. Mercury deposition in the western tropical South Atlantic during the last 70 ka. Palaeogeography, Palaeoclimatology, Palaeoecology 601, 111122. https://doi.org/10.1016/j.palaeo.2022.111122
Cohen, A., Campisano, C., Arrowsmith, R., Asrat, A., Behrensmeyer, A.K., Deino, A., Feibel, C., Hill, A., Johnson, R., Kingston, J., Lamb, H., Lowenstein, T., Noren, A., Olago, D., Owen, R.B., Potts, R., Reed, K., Renaut, R., Schäbitz, F., Tiercelin, J.-J., Trauth, M.H., Wynn, J., Ivory, S., Brady, K., O'Grady, R., Rodysill, J., Githiri, J., Russell, J., Foerster, V., Dommain, R., Rucina, S., Deocampo, D., Russell, J., Billingsley, A., Beck, C., Dorenbeck, G., Dullo, L., Feary, D., Garello, D., Gromig, R., Johnson, T., Junginger, A., Karanja, M., Kimburi, E., Mbuthia, A., McCartney, T., McNulty, E., Muiruri, V., Nambiro, E., Negash, E.W., Njagi, D., Wilson, J.N., Rabideaux, N., Raub, T., Sier, M.J., Smith, P., Urban, J., Warren, M., Yadeta, M., Yost, C., Zinaye, B., 2016. The Hominin Sites and Paleolakes Drilling Project: inferring the environmental context of human evolution from eastern African rift lake deposits. Sci. Dril. 21, 1–16. https://doi.org/10.5194/sd-21-1-2016
Cohen, A.S., Campisano, C.J., Arrowsmith, J.R., Asrat, A., Beck, C.C., Behrensmeyer, A.K., Deino, A.L., Feibel, C.S., Foerster, V., Kingston, J.D., Lamb, H.F., Lowenstein, T.K., Lupien, R.L., Muiruri, V., Olago, D.O., Owen, R.B., Potts, R., Russell, J.M., Schaebitz, F., Stone, J.R., Trauth, M.H., Yost, C.L., 2022. Reconstructing the Environmental Context of Human Origins in Eastern Africa Through Scientific Drilling. Annu. Rev. Earth Planet. Sci. 50, 451–476. https://doi.org/10.1146/annurev-earth-031920-081947
Cohen, A.S., Stone, J.R., Beuning, K.R.M., Park, L.E., Reinthal, P.N., Dettman, D., Scholz, C.A., Johnson, T.C., King, J.W., Talbot, M.R., Brown, E.T., Ivory, S.J., 2007. Ecological consequences of early Late Pleistocene megadroughts in tropical Africa. Proc. Natl. Acad. Sci. U.S.A. 104, 16422–16427. https://doi.org/10.1073/pnas.0703873104
Cooke, C.A., Martínez-Cortizas, A., Bindler, R., Sexauer Gustin, M., 2020. Environmental archives of atmospheric Hg deposition – A review. Science of the Total Environment 709, 134800. https://doi.org/10.1016/j.scitotenv.2019.134800
Crocker, A.J., Naafs, B.D.A., Westerhold, T., James, R.H., Cooper, M.J., Röhl, U., Pancost, R.D., Xuan, C., Osborne, C.P., Beerling, D.J., Wilson, P.A., 2022. Astronomically controlled aridity in the Sahara since at least 11 million years ago. Nat. Geosci. 15, 671–676. https://doi.org/10.1038/s41561-022-00990-7
deMenocal, P.B., 1995. Plio-Pleistocene African Climate. Science 270, 53–59. https://doi.org/10.1126/science.270.5233.53
Deplazes, G., Lückge, A., Peterson, L.C., Timmermann, A., Hamann, Y., Hughen, K.A., Röhl, U., Laj, C., Cane, M.A., Sigman, D.M., Haug, G.H., 2013. Links between tropical rainfall and North Atlantic climate during the last glacial period. Nature Geoscience 6, 213–217. https://doi.org/10.1038/ngeo1712
Edwards, B.A., Kushner, D.S., Outridge, P.M., Wang, F., 2021. Fifty years of volcanic mercury emission research: Knowledge gaps and future directions. Science of the Total Environment 757, 143800. https://doi.org/10.1016/j.scitotenv.2020.143800

Engstrom, D.R., Rose, N.L., 2013. A whole-basin, mass-balance approach to paleolimnology. J Paleolimnol 49, 333–347. https://doi.org/10.1007/s10933-012-9675-5
Fadina, O.A., Venancio, I.M., Belem, A., Silveira, C.S., Bertagnolli, D. de C., Silva-Filho, E.V., Albuquerque, A.L.S., 2019. Paleoclimatic controls on mercury deposition in northeast Brazil since the Last Interglacial. Quaternary Science Reviews 221, 105869. https://doi.org/10.1016/j.quascirev.2019.105869
Figueiredo, T.S., Bergquist, B.A., Santos, T.P., Albuquerque, A.L.S., Silva-Filho, E.V., 2022. Relationship between glacial CO2 drawdown and mercury cycling in the western South Atlantic: An isotopic insight. Geology 50, 3–7. https://doi.org/10.1130/g49942.1
Foerster, V., Asrat, A., Bronk Ramsey, C., Brown, E.T., Chapot, M.S., Deino, A., Duesing, W., Grove, M., Hahn, A., Junginger, A., Kaboth-Bahr, S., Lane, C.S., Opitz, S., Noren, A., Roberts, H.M., Stockhecke, M., Tiedemann, R., Vidal, C.M., Vogelsang, R., Cohen, A.S., Lamb, H.F., Schaebitz, F., Trauth, M.H., 2022. Pleistocene climate variability in eastern Africa influenced hominin evolution. Nat. Geosci. 15, 805–811. https://doi.org/10.1038/s41561-022-01032-y
Francisco López, A., Heckenauer Barrón, E.G., Bello Bugallo, P.M., 2022. Contribution to understanding the influence of fires on the mercury cycle: Systematic review, dynamic modelling and application to sustainable hypothetical scenarios. Environ Monit Assess 194, 707. https://doi.org/10.1007/s10661-022-10208-3
Frieling, J., Mather, T.A., März, C., Jenkyns, H.C., Hennekam, R., Reichart, G.-J., Slomp, C.P., Van Helmond, N.A.G.M., 2023. Effects of redox variability and early diagenesis on marine sedimentary Hg records. Geochimica et Cosmochimica Acta S0016703723001850. https://doi.org/10.1016/j.gca.2023.04.015
Gao, X., Yuan, W., Chen, J., Huang, F., Wang, Z., Gong, Y., Zhang, Y., Liu, Y., Zhang, T., Zheng, W., 2023. Tracing the source and transport of Hg during pedogenesis in strongly weathered tropical soil using Hg isotopes. Geochimica et Cosmochimica Acta 361, 101–112. https://doi.org/10.1016/j.gca.2023.10.009
Gehrke, G.E., Blum, J.D., Meyers, P.A., 2009. The geochemical behavior and isotopic composition of Hg in a mid-Pleistocene western Mediterranean sapropel. Geochimica et Cosmochimica Acta 73, 1651–1665. https://doi.org/10.1016/j.gca.2008.12.012
Gosling, W.D., McMichael, C.N.H., Groenwoud, Z., Roding, E., Miller, C.S., Julier, A.C.M., 2021. Preliminary evidence for green, brown and black worlds in tropical western Africa during the Middle and Late Pleistocene. Palaeoecology of Africa 35, 13–25. https://doi.org/10.1201/9781003162766
Gosling, W.D., Miller, C.S., Shanahan, T.M., Holden, P.B., Overpeck, J.T., van Langevelde, Frank., 2022a. A stronger role for long-term moisture change than for CO2 in determining tropical woody vegetation change. Science 376, 653–656. https://doi.org/10.1126/science.abg4618
Gosling, W.D., Scerri, E.M.L., Kaboth-Bahr, S., 2022b. The climate and vegetation backdrop to hominin evolution in Africa. Philosophical Transactions of the Royal Society B: Biological Sciences 377. https://doi.org/10.1098/rstb.2020.0483
Grant, K.M., Amarathunga, U., Amies, J.D., Hu, P., Qian, Y., Penny, T., Rodriguez-Sanz, L., Zhao, X., Heslop, D., Liebrand, D., Hennekam, R., Westerhold, T., Gilmore, S., Lourens, L.J., Roberts, A.P., Rohling, E.J., 2022. Organic carbon burial in Mediterranean sapropels intensified during Green Sahara Periods since 3.2 Myr ago. Commun Earth Environ 3, 11. https://doi.org/10.1038/s43247-021-00339-9
Grant, K.M., Grimm, R., Mikolajewicz, U., Marino, G., Ziegler, M., Rohling, E.J., 2016. The timing of Mediterranean sapropel deposition relative to insolation, sea-level and African monsoon changes. Quaternary Science Reviews 140, 125–141. https://doi.org/10.1016/j.quascirev.2016.03.026
Grant, K.M., Rohling, E.J., Westerhold, T., Zabel, M., Heslop, D., Konijnendijk, T., Lourens, L., 2017. A 3 million year index for North African humidity/aridity and the implication of potential pan-African Humid periods. Quaternary Science Reviews 171, 100–118. https://doi.org/10.1016/j.quascirev.2017.07.005
Grygar, T.M., Mach, K., Martinez, M., 2019. Checklist for the use of potassium concentrations in siliciclastic sediments as paleoenvironmental archives. Sedimentary Geology 382, 75–84. https://doi.org/10.1016/j.sedgeo.2019.01.010
Guédron, S., Ledru, M.P., Escobar-Torrez, K., Develle, A.L., Brisset, E., 2018. Enhanced mercury deposition by Amazonian orographic precipitation: Evidence from high-elevation Holocene records of the Lake Titicaca region (Bolivia). Palaeogeography, Palaeoclimatology, Palaeoecology 511, 577–587. https://doi.org/10.1016/j.palaeo.2018.09.023
Gulati, R.D., Zadereev, E.S., Degermendzhi, A.G. (Eds.), 2017. Ecology of Meromictic Lakes, Ecological Studies. Springer International Publishing, Cham. https://doi.org/10.1007/978-3-319-49143-1
Gustin, M.S., Bank, M.S., Bishop, K., Bowman, K., Branfireun, B., Chételat, J., Eckley, C.S., Hammerschmidt, C.R., Lamborg, C., Lyman, S., Martínez-Cortizas, A., Sommar, J., Tsui, M.T.-K., Zhang, T., 2020. Mercury biogeochemical cycling: A synthesis of recent scientific advances. Science of The Total Environment 737, 139619. https://doi.org/10.1016/j.scitotenv.2020.139619
Ha, J., Zhao, X., Yu, R., Barkay, T., Yee, N., 2017. Hg(II) reduction by siderite ($FeCO_3$). Applied Geochemistry 78, 211-218. https://doi.org/10.1016/j.apgeochem.2016.12.017
Hammer, Ø., Harper, D.A.T., Ryan, P.D., 2001. PAST: Paleontological statistics software package for education and data analysis. Palaeontologia Electronica 4, 9.
Han, S., Obraztsova, A., Pretto, P., Deheyn, D.D., Gieskes, J., Tebo, B.M., 2008. Sulfide and iron control on mercury speciation in anoxic estuarine sediment slurries. Marine Chemistry 111, 214–220. https://doi.org/10.1016/j.marchem.2008.05.002

Hermanns, Y.M., Biester, H., 2013. A 17,300-year record of mercury accumulation in a pristine lake in southern Chile. Journal of Paleolimnology 49, 547–561. https://doi.org/10.1007/s10933-012-9668-4
Hermanns, Y.M., Cortizas, A.M., Arz, H., Stein, R., Biester, H., 2013. Untangling the influence of in-lake productivity and terrestrial organic matter flux on 4,250 years of mercury accumulation in Lake Hambre, Southern Chile. Journal of Paleolimnology 49, 563–573. https://doi.org/10.1007/s10933-012-9657-7
Hernández, A., Martin-Puertas, C., Moffa-Sánchez, P., Moreno-Chamarro, E., Ortega, P., Blockley, S., Cobb, K., Comas-Bru, L., Giralt, S., Goosse, H., Luterbacher, J., Martrat, B., Muscheler, R., Parnell, A., Pla-Rabes, S., Sjolte, J., Scaife, A., Swingedouw, D., Wise, E., Xu, G., 2020. Modes of climate variability: Synthesis and review of proxy-based reconstructions through the Holocene. Earth-Science Reviews 209, 103286. https://doi.org/10.1016/j.earscirev.2020.103286
Hsu-Kim, H., Kucharzyk, K.H., Zhang, T., Deshusses, M.A., 2013. Mechanisms Regulating Mercury Bioavailability for Methylating Microorganisms in the Aquatic Environment: A Critical Review. Environ. Sci. Technol. 47, 2441–2456. https://doi.org/10.1021/es304370g
Jenkyns, H.C., 1988. The Early Toarcian (Jurassic) Anoxic Event. American Journal of Science.
Jenkyns, H.C., Weedon, G.P., 2013. Chemostratigraphy (CaCO3, TOC, δ13Corg) of Sinemurian (Lower Jurassic) black shales from the Wessex Basin, Dorset and palaeoenvironmental implications. nos 46, 1–21. https://doi.org/10.1127/0078-0421/2013/0029
Jeon, B., Scircle, A., Cizdziel, J.V., Chen, J., Black, O., Wallace, D.J., Zhou, Y., Lepak, R.F., Hurley, J.P., 2020. Historical deposition of trace metals in a marine sapropel from Mangrove Lake, Bermuda with emphasis on mercury, lead, and their isotopic composition. J Soils Sediments 20, 2266–2276. https://doi.org/10.1007/s11368-020-02567-6
Jones, W.B., Bacon, M., Hastings, D.A., 1981. The Lake Bosumtwi impact crater, Ghana. Geological Society of America Bulletin 92, 342–349. https://doi.org/10.1130/0016-7606(1981)92<342:TLBICG>2.0.CO;2
Jourdan, F., Renne, P.R., Reimold, W.U., 2009. An appraisal of the ages of terrestrial impact structures. Earth and Planetary Science Letters 286, 1–13. https://doi.org/10.1016/j.epsl.2009.07.009
Kaboth-Bahr, S., Gosling, W.D., Vogelsang, R., Bahr, A., Scerri, E.M.L., 2021. Paleo-ENSO influence on African environments and early modern humans. Proceedings of the National Academy of Science 118, 1–6. https://doi.org/10.1073/pnas.2018277118
Karp, A.T., Uno, K.T., Berke, M.A., Russell, J.M., Scholz, C.A., Marlon, J.R., Faith, J.T., Staver, A.C., 2023. Nonlinear rainfall effects on savanna fire activity across the African Humid Period. Quaternary Science Reviews 304, 107994. https://doi.org/10.1016/j.quascirev.2023.107994
Kiely, R., 2023. A 50,000-year reconstruction of West African fire history (MSc Thesis). University of Amsterdam, Amsterdam.
Kinsley, C.W., Bradtmiller, L.I., McGee, D., Galgay, M., Stuut, J.B., Tjallingii, R., Winckler, G., DeMenocal, P.B., 2022. Orbital and Millennial-Scale Variability in Northwest African Dust Emissions Over the Past 67,000 years. Paleoceanography and Paleoclimatology 37, 1–22. https://doi.org/10.1029/2020PA004137
Koeberl, C., Milkereit, B., Overpeck, J.T., Scholz, C.A., Amoako, P.Y.O., Boamah, D., Danuor, S.K., Karp, T., Kueck, J., Hecky, R.E., King, J.W., Peack, J.A., 2007. An international and multidisciplinary drilling project into a young complex impact structure: The 2004 ICDP Bosumtwi Crater Drilling Project - An overview. Meteoritics and Planetary Science 42, 483–511. https://doi.org/10.1111/j.1945-5100.2007.tb01057.x
Koeberl, C., Peck, J., King, J., Milkereit, B., Overpeck, J., Scholz, C., 2005. The ICDP lake Bosumtwi drilling project: A first report. Scientific Drilling 1, 23–27. https://doi.org/10.2204/iodp.sd.1.04.2005
Kuechler, R.R., Schefuß, E., Beckmann, B., Dupont, L., Wefer, G., 2013. NW African hydrology and vegetation during the Last Glacial cycle reflected in plant-wax-specific hydrogen and carbon isotopes. Quaternary Science Reviews 82, 56–67. https://doi.org/10.1016/j.quascirev.2013.10.013
Kuss, J., Zülicke, C., Pohl, C., Schneider, B., 2011. Atlantic mercury emission determined from continuous analysis of the elemental mercury sea-air concentration difference within transects between 50°N and 50°S. Global Biogeochem. Cycles 25. https://doi.org/10.1029/2010GB003998
Larrasoaña, J.C., Roberts, A.P., Rohling, E.J., 2013. Dynamics of Green Sahara Periods and Their Role in Hominin Evolution. PLoS ONE 8. https://doi.org/10.1371/journal.pone.0076514
Laskar, J., Robutel, P., Joutel, F., Gastineau, M., Correia, A.C.M., Levrard, B., 2004. A long-term numerical solution for the insolation quantities of the Earth. Astronomy and Astrophysics 428, 261–285. https://doi.org/10.1051/0004-6361:20041335
Leiva González, J., Diaz-Robles, L.A., Cereceda-Balic, F., Pino-Cortés, E., Campos, V., 2022. Atmospheric Modelling of Mercury in the Southern Hemisphere and Future Research Needs: A Review. Atmosphere 13, 1226. https://doi.org/10.3390/atmos13081226
Lent, R.M., Alexander, C.R., 1996. Mercury accumulation in Devils Lake, north Dakota - effects of environmental variation in closed-basin lakes on mercury chronologies. Water, Air, & Soil Pollution 98, 275–296.
Lézine, A.-M., Izumi, K., Kageyama, M., Achoundong, G., 2019. A 90,000-year record of Afromontane forest responses to climate change. Science 363, 177–181. https://doi.org/10.1126/science.aav6821
Li, F., Ma, C., Zhang, P., 2020. Mercury Deposition, Climate Change and Anthropogenic Activities: A Review. Frontiers in Earth Science 8, 316. https://doi.org/10.3389/feart.2020.00316
Lisiecki, L.E., Raymo, M.E., 2005a. A Pliocene-Pleistocene stack of 57 globally distributed benthic δ 18O records. Paleoceanography 20, 1–17. https://doi.org/10.1029/2004PA001071
Lisiecki, L.E., Raymo, M.E., 2005b. A Pliocene-Pleistocene stack of 57 globally distributed benthic δ 18O records. Paleoceanography 20, 1–17. https://doi.org/10.1029/2004PA001071

Liu, M., Zhang, Q., Maavara, T., Liu, S., Wang, X., Raymond, P.A., 2021. Rivers as the largest source of mercury to coastal oceans worldwide. Nature Geoscience 14, 672–677. https://doi.org/10.1038/s41561-021-00793-2

Lupien, R., Uno, K., Rose, C., deRoberts, N., Hazan, C., De Menocal, P., Polissar, P., 2023. Low-frequency orbital variations controlled climatic and environmental cycles, amplitudes, and trends in northeast Africa during the Plio-Pleistocene. Commun Earth Environ 4, 360. https://doi.org/10.1038/s43247-023-01034-7

Lyman, S.N., Cheng, I., Gratz, L.E., Weiss-Penzias, P., Zhang, L., 2020. An updated review of atmospheric mercury. Science of the Total Environment 707, 135575. https://doi.org/10.1016/j.scitotenv.2019.135575

Machado, W., Sanders, C.J., Santos, I.R., Sanders, L.M., Silva-Filho, E.V., Luiz-Silva, W., 2016. Mercury dilution by autochthonous organic matter in a fertilized mangrove wetland. Environmental Pollution 213, 30–35. https://doi.org/10.1016/j.envpol.2016.02.002

Mason, R.P., Laporte, J.M., Andres, S., 2000. Factors controlling the bioaccumulation of mercury, methylmercury, arsenic, selenium, and cadmium by freshwater invertebrates and fish. Archives of Environmental Contamination and Toxicology 38, 283–297. https://doi.org/10.1007/s002449910038

McKay, N.P., 2012. A multidisciplinary approach to late Quaternary paleoclimatology with an emphasis on sub-saharan West Africa and the last interglacial period (PhD Thesis). University of Arizona, Arizona.

Menviel, L., Govin, A., Avenas, A., Meissner, K.J., Grant, K.M., Tzedakis, P.C., 2021. Drivers of the evolution and amplitude of African Humid Periods. Commun Earth Environ 2, 237. https://doi.org/10.1038/s43247-021-00309-1

Miller, C.S., Gosling, W.D., 2014. Quaternary forest associations in lowland tropical West Africa. Quaternary Science Reviews 84, 7–25. https://doi.org/10.1016/j.quascirev.2013.10.027

Miller, C.S., Gosling, W.D., Kemp, D.B., Coe, A.L., Gilmour, I., 2016. Drivers of ecosystem and climate change in tropical West Africa over the past ~540 000 years. Journal of Quaternary Science 31, 671–677. https://doi.org/10.1002/jqs.2893

Nalbant, J., Schneider, L., Hamilton, R., Connor, S., Biester, H., Stuart-Williams, H., Bergal-Kuvikas, O., Jacobsen, G., Stevenson, J., 2023. Fire, volcanism and climate change: the main factors controlling mercury (Hg) accumulation rates in Tropical Lake Lantoa, Sulawesi, Indonesia (~16,500–540 cal yr BP). Front. Environ. Chem. 4, 1241176. https://doi.org/10.3389/fenvc.2023.1241176

Nicholson, S.E., 2013. The West African Sahel: A Review of Recent Studies on the Rainfall Regime and Its Interannual Variability. ISRN Meteorology 2013, 1–32. https://doi.org/10.1155/2013/453521

Obrist, D., Kirk, J.L., Zhang, L., Sunderland, E.M., Jiskra, M., Selin, N.E., 2018. A review of global environmental mercury processes in response to human and natural perturbations: Changes of emissions, climate, and land use. Ambio 47, 116–140. https://doi.org/10.1007/s13280-017-1004-9

O'Mara, N.A., Skonieczny, C., McGee, D., Winckler, G., Bory, A.J.-M., Bradtmiller, L.I., Malaizé, B., Polissar, P.J., 2022. Pleistocene drivers of Northwest African hydroclimate and vegetation. Nat Commun 13, 3552. https://doi.org/10.1038/s41467-022-31120-x

Outridge, P.M., Stern, G.A., Hamilton, P.B., Sanei, H., 2019. Algal scavenging of mercury in preindustrial Arctic lakes. Limnol Oceanogr 64, 1558–1571. https://doi.org/10.1002/lno.11135

Outridge, Sanei, H., Stern, Hamilton, Goodarzi, F., 2007. Evidence for Control of Mercury Accumulation Rates in Canadian High Arctic Lake Sediments by Variations of Aquatic Primary Productivity. Environ. Sci. Technol. 41, 5259–5265. https://doi.org/10.1021/es070408x

Paine, A.R., Fendley, I.M., Frieling, J., Mather, T.A., Lacey, J.H., Wagner, B., Robinson, S.A., Pyle, D.M., Francke, A., Them II, T.R., Panagiotopoulos, K., 2024. Mercury records covering the past 90 000 years from lakes Prespa and Ohrid, SE Europe. Biogeosciences 21, 531–556. https://doi.org/10.5194/bg-21-531-2024

Pan, J., Zhong, W., Wei, Z., Ouyang, J., Shang, S., Ye, S., Chen, Y., Xue, J., Tang, X., 2020. A 15,400-year record of natural and anthropogenic input of mercury (Hg) in a sub-alpine lacustrine sediment succession from the western Nanling Mountains, South China. Environmental Science and Pollution Research 27, 20478–20489. https://doi.org/10.1007/s11356-020-08421-z

Pausata, F.S.R., Gaetani, M., Messori, G., Berg, A., Maia de Souza, D., Sage, R.F., deMenocal, P.B., 2020. The Greening of the Sahara: Past Changes and Future Implications. One Earth 2, 235–250. https://doi.org/10.1016/j.oneear.2020.03.002

Peck, J.A., Green, R.R., Shanahan, T., King, J.W., Overpeck, J.T., Scholz, C.A., 2004. A magnetic mineral record of Late Quaternary tropical climate variability from Lake Bosumtwi, Ghana. Palaeogeography, Palaeoclimatology, Palaeoecology 215, 37–57. https://doi.org/10.1016/j.palaeo.2004.08.003

Pérez-Rodríguez, M., Margalef, O., Corella, J.P., Saiz-Lopez, A., Pla-Rabes, S., Giralt, S., Cortizas, A.M., 2018. The role of climate: 71 ka of atmospheric mercury deposition in the southern hemisphere recorded by Rano Aroi Mire, Easter Island (Chile). Geosciences (Switzerland) 8. https://doi.org/10.3390/geosciences8100374

Pilla, R.M., Williamson, C.E., Adamovich, B.V., Adrian, R., Anneville, O., Chandra, S., Colom-Montero, W., Devlin, S.P., Dix, M.A., Dokulil, M.T., Gaiser, E.E., Girdner, S.F., Hambright, K.D., Hamilton, D.P., Havens, K., Hessen, D.O., Higgins, S.N., Huttula, T.H., Huuskonen, H., Isles, P.D.F., Joehnk, K.D., Jones, I.D., Keller, W.B., Knoll, L.B., Korhonen, J., Kraemer, B.M., Leavitt, P.R., Lepori, F., Luger, M.S., Maberly, S.C., Melack, J.M., Melles, S.J., Müller-Navarra, D.C., Pierson, D.C., Pislegina, H.V., Plisnier, P.-D., Richardson, D.C., Rimmer, A., Rogora, M., Rusak, J.A., Sadro, S., Salmaso, N., Saros, J.E., Saulnier-Talbot, É., Schindler, D.E., Schmid, M., Shimaraeva, S.V., Silow, E.A., Sitoki, L.M., Sommaruga, R., Straile, D., Strock, K.E., Thiery, W., Timofeyev, M.A., Verburg, P., Vinebrooke, R.D.,

Weyhenmeyer, G.A., Zadereev, E., 2020. Deeper waters are changing less consistently than surface waters in a global analysis of 102 lakes. Sci Rep 10, 20514. https://doi.org/10.1038/s41598-020-76873-x
Pompeani, D.P., Cooke, C.A., Abbott, M.B., Drevnick, P.E., 2018. Climate, Fire, and Vegetation Mediate Mercury Delivery to Midlatitude Lakes over the Holocene. Environmental Science and Technology 52, 8157–8164. https://doi.org/10.1021/acs.est.8b01523
Ravichandran, M., 2004. Interactions between mercury and dissolved organic matter - A review. Chemosphere 55, 319–331. https://doi.org/10.1016/j.chemosphere.2003.11.011
Russell, J., Talbot, M.R., Haskell, B.J., 2003. Mid-holocene climate change in Lake Bosumtwi, Ghana. Quaternary Research 60, 133–141. https://doi.org/10.1016/S0033-5894(03)00065-6
Sanei, H., Grasby, S., Beauchamp, B., 2012. Latest Permian mercury anomalies. Geology 40, 63–66.
Schneider, L., Cooke, C.A., Stansell, N.D., Haberle, S.G., 2020. Effects of climate variability on mercury deposition during the Older Dryas and Younger Dryas in the Venezuelan Andes. Journal of Paleolimnology 63, 211–224. https://doi.org/10.1007/s10933-020-00111-7
Schneider, L., Fisher, J.A., Diéguez, M.C., Fostier, A.-H., Guimaraes, J.R.D., Leaner, J.J., Mason, R., 2023. A synthesis of mercury research in the Southern Hemisphere, part 1: Natural processes. Ambio 52, 897–917. https://doi.org/10.1007/s13280-023-01832-5
Scholz, C.A., Johnson, T.C., Cohen, A.S., King, J.W., Peck, J.A., Overpeck, J.T., Talbot, M.R., Brown, E.T., Kalindekafe, L., Amoako, P.Y.O., Lyons, R.P., Shanahan, T.M., Castañeda, I.S., Heil, C.W., Forman, S.L., McHargue, L.R., Beuning, K.R., Gomez, J., Pierson, J., 2007. East African megadroughts between 135 and 75 thousand years ago and bearing on early-modern human origins. Proceedings of the National Academy of Sciences of the United States of America 104, 16416–16421. https://doi.org/10.1073/pnas.0703874104
Schultze, M., Boehrer, B., Wendt-Potthoff, K., Katsev, S., Brown, E.T., 2017. Chemical Setting and Biogeochemical Reactions in Meromictic Lakes, in: Ecology of Meromictic Lakes. Springer, pp. 35–61.
Schütze, M., Gatz, P., Gilfedder, B., Biester, H., 2021. Why productive lakes are larger mercury sedimentary sinks than oligotrophic brown water lakes. Limnol Oceanogr 66, 1316–1332. https://doi.org/10.1002/lno.11684
Schütze, M., Tserendorj, G., Pérez-Rodríguez, M., Rösch, M., Biester, H., 2018. Prediction of Holocene mercury accumulation trends by combining palynological and geochemical records of lake sediments (Black Forest, Germany). Geosciences (Switzerland) 8. https://doi.org/10.3390/geosciences8100358
Sebag, D., Garcin, Y., Adatte, T., Deschamps, P., Ménot, G., Verrecchia, E.P., 2018. Correction for the siderite effect on Rock-Eval parameters: Application to the sediments of Lake Barombi (southwest Cameroon). Organic Geochemistry 123, 126–135. https://doi.org/10.1016/j.orggeochem.2018.05.010
Segato, D., Saiz-Lopez, A., Mahajan, A.S., Wang, F., Corella, J.P., Cuevas, C.A., Erhardt, T., Jensen, C.M., Zeppenfeld, C., Kjær, H.A., Turetta, C., Cairns, W.R.L., Barbante, C., Spolaor, A., 2023. Arctic mercury flux increased through the Last Glacial Termination with a warming climate. Nat. Geosci. 16, 439–445. https://doi.org/10.1038/s41561-023-01172-9
Selin, N.E., 2009. Global biogeochemical cycling of mercury: a review. Annual Review of Environmental Resources 34, 43–63.
Shanahan, T.M., Beck, J.W., Overpeck, J.T., McKay, N.P., Pigati, J.S., Peck, J.A., Scholz, C.A., Heil, C.W., King, J., 2012. Late Quaternary sedimentological and climate changes at Lake Bosumtwi Ghana: New constraints from laminae analysis and radiocarbon age modeling. Palaeogeography, Palaeoclimatology, Palaeoecology 361–362, 49–60. https://doi.org/10.1016/j.palaeo.2012.08.001
Shanahan, T.M., Mckay, N.P., Hughen, K.A., Overpeck, J.T., Otto-Bliesner, B., Heil, C.W., King, J., Scholz, C.A., Peck, J., 2015. The time-transgressive termination of the African humid period. Nature Geoscience 8, 140–144. https://doi.org/10.1038/ngeo2329
Shanahan, T.M., Overpeck, J.T., Anchukaitis, K.J., Beck, J.W., Cole, J.E., Dettman, D.L., Peck, J.A., Scholz, C.A., King, J.W., 2009. Atlantic forcing of persistent drought in West Africa. Science 324, 377–380. https://doi.org/10.1126/science.1166352
Shanahan, T.M., Overpeck, J.T., Beck, J.W., Wheeler, C.W., Peck, J.A., King, J.W., Scholz, C.A., 2008a. The formation of biogeochemical laminations in Lake Bosumtwi, Ghana, and their usefulness as indicators of past environmental changes. Journal of Paleolimnology 40, 339–355. https://doi.org/10.1007/s10933-007-9164-4
Shanahan, T.M., Overpeck, J.T., Scholz, C.A., Beck, J.W., Peck, J., King, J.W., 2008b. Abrupt changes in the water balance of tropical West Africa during the late Quaternary. J. Geophys. Res. 113, D12108. https://doi.org/10.1029/2007JD009320
Shanahan, T.M., Overpeck, J.T., Sharp, W.E., Scholz, C.A., Arko, J.A., 2007. Simulating the response of a closed-basin lake to recent climate changes in tropical West Africa (Lake Bosumtwi, Ghana). Hydrological Processes 21, 1678–1691. https://doi.org/10.1002/hyp.6359
Shanahan, T.M., Overpeck, J.T., Wheeler, C.W., Beck, J.W., Pigati, J.S., Talbot, M.R., Scholz, C.A., Peck, J., King, J.W., 2006. Paleoclimatic variations in West Africa from a record of late Pleistocene and Holocene lake level stands of Lake Bosumtwi, Ghana. Palaeogeography, Palaeoclimatology, Palaeoecology 242, 287–302. https://doi.org/10.1016/j.palaeo.2006.06.007
Shanahan, T.M., Peck, J.A., McKay, N., Heil, C.W., King, J., Forman, S.L., Hoffmann, D.L., Richards, D.A., Overpeck, J.T., Scholz, C., 2013. Age models for long lacustrine sediment records using multiple dating approaches - An example from Lake Bosumtwi, Ghana. Quaternary Geochronology 15, 47–60. https://doi.org/10.1016/j.quageo.2012.12.001

Shen, J., Feng, Q., Algeo, T.J., Liu, Jinling, Zhou, C., Wei, W., Liu, Jiangsi, Them, T.R., Gill, B.C., Chen, J., 2020. Sedimentary host phases of mercury (Hg) and implications for use of Hg as a volcanic proxy. Earth and Planetary Science Letters 543, 116333. https://doi.org/10.1016/j.epsl.2020.116333
Skonieczny, C., McGee, D., Winckler, G., Bory, A., Bradtmiller, L.I., Kinsley, C.W., Polissar, P.J., De Pol-Holz, R., Rossignol, L., Malaizé, B., 2019. Monsoon-driven Saharan dust variability over the past 240,000 years. Science Advances 5, 1–9. https://doi.org/10.1126/sciadv.aav1887
Soerensen, A.L., Mason, R.P., Balcom, P.H., Jacob, D.J., Zhang, Y., Kuss, J., Sunderland, E.M., 2014. Elemental Mercury Concentrations and Fluxes in the Tropical Atmosphere and Ocean. Environ. Sci. Technol. 48, 11312–11319. https://doi.org/10.1021/es503109p
Sprovieri, F., Pirrone, N., Bencardino, M., D'Amore, F., Angot, H., Barbante, C., Brunke, E.-G., Arcega-Cabrera, F., Cairns, W., Comero, S., Diéguez, M. del C., Dommergue, A., Ebinghaus, R., Feng, X.B., Fu, X., Garcia, P.E., Gawlik, B.M., Hageström, U., Hansson, K., Horvat, M., Kotnik, J., Labuschagne, C., Magand, O., Martin, L., Mashyanov, N., Mkololo, T., Munthe, J., Obolkin, V., Ramirez Islas, M., Sena, F., Somerset, V., Spandow, P., Vardè, M., Walters, C., Wängberg, I., Weigelt, A., Yang, X., Zhang, H., 2017. Five-year records of mercury wet deposition flux at GMOS sites in the Northern and Southern hemispheres. Atmos. Chem. Phys. 17, 2689–2708. https://doi.org/10.5194/acp-17-2689-2017
Sprovieri, F., Pirrone, N., Ebinghaus, R., Kock, H., Dommergue, A., 2010. A review of worldwide atmospheric mercury measurements. Atmospheric Chemistry and Physics 10, 8245–8265. https://doi.org/10.5194/acp-10-8245-2010
Stager, J.C., Ryves, D.B., Chase, B.M., Pausata, F.S.R., 2011. Catastrophic Drought in the Afro-Asian Monsoon Region During Heinrich Event 1. Science 331, 1299–1302. https://doi.org/10.1126/science.1198322
Swart, P.K., 2015. The geochemistry of carbonate diagenesis: The past, present and future. Sedimentology 62, 1233–1304. https://doi.org/10.1111/sed.12205
Talbot, M.R., Johannessen, T., 1992. A high resolution palaeoclimatic record for the last 27,500 years in tropical West Africa from the carbon and nitrogen isotopic composition of lacustrine organic matter. Earth and Planetary Science Letters 110, 23–37. https://doi.org/10.1016/0012-821X(92)90036-U
Them, T.R., Jagoe, C.H., Caruthers, A.H., Gill, B.C., Grasby, S.E., Gröcke, D.R., Yin, R., Owens, J.D., 2019. Terrestrial sources as the primary delivery mechanism of mercury to the oceans across the Toarcian Oceanic Anoxic Event (Early Jurassic). Earth and Planetary Science Letters 507, 62–72. https://doi.org/10.1016/j.epsl.2018.11.029
Tisserand, D., Guédron, S., Viollier, E., Jézéquel, D., Rigaud, S., Campillo, S., Sarret, G., Charlet, L., Cossa, D., 2022. Mercury, organic matter, iron, and sulfur co-cycling in a ferruginous meromictic lake. Applied Geochemistry 146, 105463. https://doi.org/10.1016/j.apgeochem.2022.105463
Tjallingii, R., Claussen, M., Stuut, J.-B.W., Fohlmeister, J., Jahn, A., Bickert, T., Lamy, F., Röhl, U., 2008. Coherent high- and low-latitude control of the northwest African hydrological balance. Nature Geosci 1, 670–675. https://doi.org/10.1038/ngeo289
Trauth, M.H., Asrat, A., Berner, N., Bibi, F., Foerster, V., Grove, M., Kaboth-Bahr, S., Maslin, M.A., Mudelsee, M., Schäbitz, F., 2021. Northern Hemisphere Glaciation, African climate and human evolution. Quaternary Science Reviews 268, 107095. https://doi.org/10.1016/j.quascirev.2021.107095
Tribovillard, N., Algeo, T.J., Lyons, T., Riboulleau, A., 2006. Trace metals as paleoredox and paleoproductivity proxies: An update. Chemical Geology 232, 12–32. https://doi.org/10.1016/j.chemgeo.2006.02.012
Turner, B.F., Gardner, L.R., Sharp, W.E., 1996. The hydrology of lake Bosumtwi, a climate-sensitive lake in Ghana, West Africa. Journal of Hydrology 183, 243–261. https://doi.org/10.1016/0022-1694(95)02982-6
United Nations Environment Programme, 2018. Global Mercury Assessment, United Nations.
Vindušková, O., Jandová, K., Frouz, J., 2019. Improved method for removing siderite by *in situ* acidification before elemental and isotope analysis of soil organic carbon. J. Plant Nutr. Soil Sci. 182, 82–91. https://doi.org/10.1002/jpln.201800164
Vinnepand, M., Zeeden, C., Wonik, T., Gosling, W., Noren, A., Kück, J., Pierdominici, S., Voigt, S., Abadi, M.S., Ulfers, A., Danour, S., Afrifa, K., Kaboth-Bahr, S., 2024. An age-depth model for Lake Bosumtwi (Ghana) to reconstruct one million years of West African climate and environmental change. Quaternary Science Reviews 325, 108478. https://doi.org/10.1016/j.quascirev.2023.108478
Weldeab, S., Lea, D.W., Schneider, R.R., Andersen, N., 2007. 155,000 Years of West African Monsoon and Ocean Thermal Evolution. Science 316, 1303–1307. https://doi.org/10.1126/science.1140461
White, F. (Frank), 1983. The vegetation of Africa: a descriptive memoir to accompany the Unesco/AETFAT/UNSO vegetation map of Africa, Natural resources research ; 20. Unesco, Paris.
Woolway, R.I., Kraemer, B.M., Lenters, J.D., Merchant, C.J., O'Reilly, C.M., Sharma, S., 2020. Global lake responses to climate change. Nature Reviews Earth and Environment 1, 388–403. https://doi.org/10.1038/s43017-020-0067-5
Yin, R., Wang, X., Sun, R., Gao, L., Deng, C., Tian, Z., Luo, A., Lehmann, B., 2024. Linking the mercury biogeochemical cycle to the deep mercury cycle: A mercury isotope perspective. Chemical Geology 654, 122063. https://doi.org/10.1016/j.chemgeo.2024.122063
Zaferani, S., Biester, H., 2021. Mercury Accumulation in Marine Sediments – A Comparison of an Upwelling Area and Two Large River Mouths. Front. Mar. Sci. 8, 732720. https://doi.org/10.3389/fmars.2021.732720
Zolitschka, B., Francus, P., Ojala, A.E.K., Schimmelmann, A., 2015. Varves in lake sediments - a review. Quaternary Science Reviews 117, 1–41.

1145 Zou, J., Chang, Y.P., Zhu, A., Chen, M.T., Kandasamy, S., Yang, H., Cui, J., Yu, P.S., Shi, X., 2021. Sedimentary
1146 mercury and antimony revealed orbital-scale dynamics of the Kuroshio Current. Quaternary Science
1147 Reviews 265, 107051. https://doi.org/10.1016/j.quascirev.2021.107051
1148